Agricultural and Forest Meteorology 313 (2022) 108755

Contents lists available at ScienceDirect

Agricultural and Forest Meteorology

journal homepage: www.elsevier.com/locate/agrformet

Testing three rainfall interception models and different parameterization methods with data from an open Mediterranean pine forest

Marinos Eliades [a,*], Adriana Bruggeman [a], Hakan Djuma [a], Andreas Christou [b], Konstantinos Rovanias [b], Maciek W. Lubczynski [c]

[a] The Cyprus Institute, Energy, Environment and Water Research Center (EEWRC), Nicosia, Cyprus
[b] Department of Forests, Ministry of Agriculture, Rural Development and Environment, Nicosia, Cyprus
[c] University of Twente, ITC, Enschede, Netherlands

ARTICLE INFO

Keywords:
Throughfall
Evaporation
Leaf Area Index
Canopy cover fraction
Canopy storage capacity
Equifinality

ABSTRACT

Various models have been developed to simulate rainfall interception by vegetation but their formulations and applications rely on a number of assumptions and parameter estimation procedures. The aim of this study is to examine the effect of different model assumptions and parameter derivation approaches on the performance of the Rutter, Gash and Liu interception models. The Rutter model, in contrast to the other two daily models, was applied both on an hourly and on a daily basis. Hourly data from a meteorological station, one automatic and 28 manual throughfall gauges from a semi-arid *Pinus brutia* forest (Cyprus) for the period between 01/Jul/2016 and 31/May/2020 were used for the analysis. We conducted a sensitivity analysis for the assessment of the model parameters and variables: canopy storage capacity (S), canopy cover fraction (c), the ratio of mean wet evaporation rate to mean wet rainfall rate ($\bar{E}_c/\bar{R}$) and potential evaporation (E_o). Three parameter derivation approaches were tested: the widely used regression method and an automatic model parameterization procedure for optimization of S and c and for optimization of S (with c observed). The parameterized models were run with daily meteorological data and compared with long-term weekly throughfall data (2008–2019). The Gash and Liu models showed low sensitivity to $\bar{E}_c/\bar{R}$. Test runs with different combinations of S, c and $\bar{E}_c/\bar{R}$ revealed strong equifinality. The models showed high performance for both calibration and validation periods with Kling–Gupta Efficiency (*KGE*) above 0.90. Gash and Liu models with the automatic model parameterization procedures resulted in higher *KGE*s than with the regression method. The interception losses computed from the long-term application of the three models ranged between 18 and 20%. The models were all capable of capturing the inherently variable interception process. However, a representative time series of throughfall measurements is needed to parameterize the models.

List of symbols

Symbol	Unit	Description
AC		Above canopy
BC		Below canopy
c		Canopy cover fraction (canopy covered area per unit ground area) =< 1.0
C_c	mm	Water storage on the canopy covered area
C_d		Mean drag coefficient
d	m	Zero plane displacement height
di	%	Relative change in interception output
dj	%	Relative change of the input parameter
D_c	mm	Drainage from the canopy covered area
E	mm	Evaporation per unit ground area
$\bar{E}$	mm h^{-1}	Mean evaporation rate under saturated conditions per unit ground area
$\bar{E}_c$	mm h^{-1}	Mean evaporation rate under saturated conditions from the canopy covered area
$\bar{E}/\bar{R}$		Mean evaporation to mean rainfall ratio
E_c	mm	Actual evaporation from the wet canopy covered area
E_o	mm	Potential wet surface evaporation per unit ground area
ET_o	mm	Reference evapotranspiration per unit ground area
h_c	m	Average tree height
I	mm	Rainfall interception per unit ground area
I_{Gash}	mm	Rainfall interception computed with the Gash model
$I_{initial}$		

(continued on next column)

(continued)

(continued on next page)

* Corresponding author.
E-mail address: m.eliades@cyi.ac.cy (M. Eliades).

https://doi.org/10.1016/j.agrformet.2021.108755
Received 7 January 2021; Received in revised form 17 November 2021; Accepted 24 November 2021
Available online 3 December 2021

(*continued*)

	% of rainfall	Rainfall interception for the initial value of a selected input parameter
I_{Liu}	mm	Rainfall interception computed with the Liu model
I_{Rutter}	mm	Rainfall interception computed with the Rutter model
I_{test}	% of rainfall	Rainfall interception for the test value of a selected input parameter
J		Input parameter value
$J_{initial}$		Initial input parameter value
J_{test}		Tested input parameter value
k		von Karman's constant (0.41)
LAI		Leaf area index
P	mm	Rainfall
p		Gap fraction
P_i	mm	Rainfall during events that saturate the canopy
P_j	mm	Rainfall during events with insufficient rain to saturate the canopy
Pn	mm/day	Average annual wet-day precipitation
P_s	mm	Amount of water needed to saturate the canopy
$P_{<2}$	mm	Rain day with less than 2 mm rain
$\bar{R}$	mm h^{-1}	Mean rainfall rate
r_a	s m^{-1}	Bulk aerodynamic resistance
RS		Relative sensitivity
S	mm	Canopy storage capacity per unit ground area
S_c	mm	Canopy storage capacity per unit area of canopy cover (S/c)
TF	mm	Throughfall per unit ground area
TF_{Gash}	mm	Throughfall computed with the Gash model
TF_{Liu}	mm	Throughfall computed with the Liu model
TF_{Rutter}	mm	Throughfall computed with the Rutter model
u	m s^{-1}	Wind speed
z	m	Reference height
z_0	m	Roughness length of the canopy
z_c	m	Roughness length for a closed canopy
γ	kPa $°C^{-1}$	Psychometric constant
Δ	kPa $°C^{-1}$	Slope of saturation vapour pressure curve
λ	MJ kg^{-1}	Latent heat of vaporization of water
ρ_a	kg m^{-3}	Density of dry air

1. Introduction

The largest water balance component of the terrestrial rainfall redistribution is evapotranspiration, which can be separated in three distinct processes: transpiration through the stomata of plants, evaporation from the soil surface and evaporation from the rainfall intercepted by the plants' surfaces (Kool et al., 2014). The vegetation type and meteorological conditions determine the amount of precipitation that will evaporate from the canopy surface (interception), flow to the ground via trunks or stems (stemflow) and fall to the ground between the various components of the vegetation (throughfall) (Crockford and Richardson, 2000). Observations show that rainfall interception is a highly variable hydrological process, ranging from 6% of the gross rainfall in savannahs to 45% of the gross rainfall in dense forests (Alavi et al., 2001; Carlyle-Moses and Gash, 2011; Llorens and Domingo, 2007; Pereira et al., 2009).

Interception losses can be estimated by empirically deriving relationships between rainfall and throughfall (e.g., M. Eliades et al., 2018; Shachnovich et al., 2008). However, these relationships cannot be applied in areas with different vegetation and meteorological conditions. A number of process-based rainfall interception models have been developed over the past few decades to overcome these limitations. The Rutter, Gash and Liu models are the rainfall interception models most commonly used in interception studies (Linhoss and Siegert, 2020, 2016; Návar, 2017).

The Rutter model uses a running canopy water balance to compute throughfall (TF), evaporation (E) and changes in canopy water storage (Rutter et al., 1971). Adaptations and modifications of the canopy drainage and of the canopy and trunk evaporation components in the Rutter model were introduced by Valente et al. (1997) for a more realistic representation of the rainfall interception process in sparse forests. The main disadvantage of the Rutter model is that it requires hourly (or higher resolution) meteorological data that are often not available.

The Gash model is a simplification of the Rutter model with a primary assumption that rainfall can be represented as a series of discrete storms, separated by intervals sufficiently long for the canopy and stems to dry completely (Gash, 1979). The Gash model as well as a number of other interception papers assumes that the ratio of the mean evaporation rate ($\bar{E}$) to the mean rainfall rate ($\bar{R}$) during saturated canopy conditions is constant (Gash, 1979; Návar, 2019). The original Gash model was corrected for a consistent formulation of the canopy cover fraction (c), and generally referred to as the revised version (Gash et al., 1995; Valente et al., 1997). The mean evaporation rate per unit ground area ($\bar{E}$) used in the original model version is calculated as $\bar{E} = c\,\bar{E}_c$ in the revised version, where $\bar{E}_c$ represents the mean evaporation rate from the canopy covered area.

The Liu model (Liu, 1997) is also a simplification of the Rutter model, but differs in the derivation of the change of canopy storage. In the Liu model, the change of throughfall is assumed to be positively proportional to rainfall intensity, canopy dryness index and the time interval between two storms (Liu, 2001; 1997). The Liu model has been corrected by Carlyle-Moses and Price (2007) to improve the simulation of interception losses in sparse forests, because the gap fraction was not included in the evaporation component of the original formulation of the model (Liu, 2001).

The revised versions of the Rutter, Gash and Liu models require the knowledge of two canopy-related parameters, the canopy storage capacity (S) and the canopy cover fraction (c) (Muzylo et al., 2009). The canopy cover fraction (c) can be quantified with optical methods in the field (Carlyle-Moses and Price, 2007; Limousin et al., 2008). The canopy storage capacity (S) is, however, more difficult to measure. It can be determined by signal attenuation methods, such as microwave, gamma ray and cosmic ray attenuation but this has been done in a very small number of studies (e.g., Bouten et al., 1996). However, as pointed out by Friesen et al. (2015), measurements with these methods may include errors related to water contained within the living tissues of the plants. Also, S can be determined by measuring mass changes of foliage components or of whole trees, but these techniques are usually destructive and limited by the size of the sample (e.g., Licata et al., 2011; Llorens and Gallart, 2000). These models also represent stemflow, which is described by the trunk storage capacity (S_t) and a drainage partitioning coefficient (p_d) (Valente et al., 1997).

The most common method for the derivation of S and c is with regression-based approaches between rainfall and throughfall (Jackson, 1975; Klaassen et al., 1998; Sadeghi et al., 2015). The 'mean' method, which is based on the least square fitting of data, has the advantage over other methods that it can provide estimates of all parameters of the Gash and Liu models (S, c and $\bar{E}/\bar{R}$). However, in many studies in sparse forests c was not considered during the derivation of S and $\bar{E}/\bar{R}$ (Sadeghi et al., 2015). The derivation of model parameters with the regression method depends on the discretization of time in storm events and dry intervals. The minimum duration of the dry interval should be sufficient to dry the vegetation. The selection of the time separation interval is often subjective; and durations in the literature vary from 2 h to 12 h (Hassan et al., 2017; Klaassen et al., 1998). The selection of a short storm event separation interval will result in more storms of short duration, thus mean rainfall and evaporation rates will be overestimated (van Dijk et al., 2015; Wallace and McJannet, 2008). Even though an event separation interval is used for model parameter derivation, many studies subsequently compute interception losses on a daily basis (e.g., Hassan et al., 2017; Ghimire et al., 2017), following the assumption of Gash (1979) that the canopy is dry at the start of each daily rainfall event.

The mean evaporation rate ($\bar{E}$) and the mean rainfall rate ($\bar{R}$) under saturated conditions can also be computed from hourly meteorological data. Gash (1979) selected a rainfall rate threshold ($\bar{R}_{sat}$) of 0.5 mm h^{-1} above which the canopy remains saturated. The author found that the $\bar{E}$ (0.19 mm h^{-1}) computed with this threshold was the same as the $\bar{E}$ derived from Bowen ratio measurements during saturated canopy

conditions at the same site by Stewart (1977). Gash (1979) also showed that $\bar{E}$ was not very sensitive to the selection of this threshold. A number of studies adopted this threshold value to compute the parameters $\bar{E}$ and $\bar{R}$, but without testing its effect on interception losses (e.g., Fernandes et al., 2017; Schellekens et al., 1999). Recently, Návar (2019) devised an independent approach based on dripping equations to evaluate both $\bar{E}$ and $\bar{R}$, using daily data of rainfall, throughfall and stemflow from 45 interception case studies in Mexico. He found that $\bar{E}$ decreased with rainfall duration but increased as a function of $\bar{R}$.

Studies on the sensitivity of the Rutter, Gash and Liu models have found a higher sensitivity of the models to c than to S in Mediterranean pine and oak forests (Limousin et al., 2008; Llorens, 1997; Mużyło et al., 2012; Valente et al., 1997). On the contrary, low sensitivity of the Gash model to c has been found for *Robinia pseudoacacia* in a semi-arid climate (Ma et al., 2020) and for *Daphniphyllum macropodum* in a subtropical, humid climate (Wei et al., 2020). As mentioned by van Dijk et al. (2015), several parameter sets of S and E may result in similar model responses, revealing collinearity. This is an important issue that needs further revision of methods to evaluate E (Návar, 2020; van Dijk et al., 2015). The term "equifinality" is used to describe these "non-unique" parameter sets (Beven, 2012). We have found no studies that analysed the equifinality between the parameters of the Rutter, Gash and Liu models.

The aim of this study is to investigate different parameter derivation approaches and model assumptions of three commonly used interception models (Rutter, Gash, Liu). We test the Rutter model both with hourly and daily data; which is the first application of the Rutter model with a daily time step in the current scientific literature. The specific objectives of this study are: (a) to examine the sensitivity of the rainfall interception models to changes of S, c and E_o or $\bar{E}_c/\bar{R}$; (b) to analyse the effect of model assumptions related to the computation of evaporation, rainfall rate threshold and event separation interval; (c) to evaluate the effects of the following model parameter derivation approaches on the computed interception: i) rainfall-throughfall regression (*regression*) for the derivation of S, c and $\bar{E}_c/\bar{R}$; ii) optimization of S and c (*optimization-S, c*) and iii) optimization of S with measured c (*optimization-S*); and (d) to compare the performances of the hourly and daily Rutter model and the daily Gash and Liu model.

The model assumptions, sensitivity and parameter derivation were analysed with hourly meteorological, rainfall and throughfall data from an open, semi-arid *Pinus brutia* forest in Cyprus, for the period between 13/Jul/2016 and 31/May/2020. The three model parameterization procedures were applied on a daily basis and their results were compared with an independent 12-year dataset (2008 – 2019) with weekly throughfall observations from the same site.

2. Materials and methods

2.1. Study area and data collection

2.1.1. Study area description

Our study was conducted in the Agia-Marina-Xyliatou forestry site from 01/Jan/2008 to 31/May/2020, within a fenced stand of *P. brutia* forest, on the northern foothills of the Troodos Mountains in Cyprus (Fig. 1, Supplementary material, Fig. S1). The study area is part of the

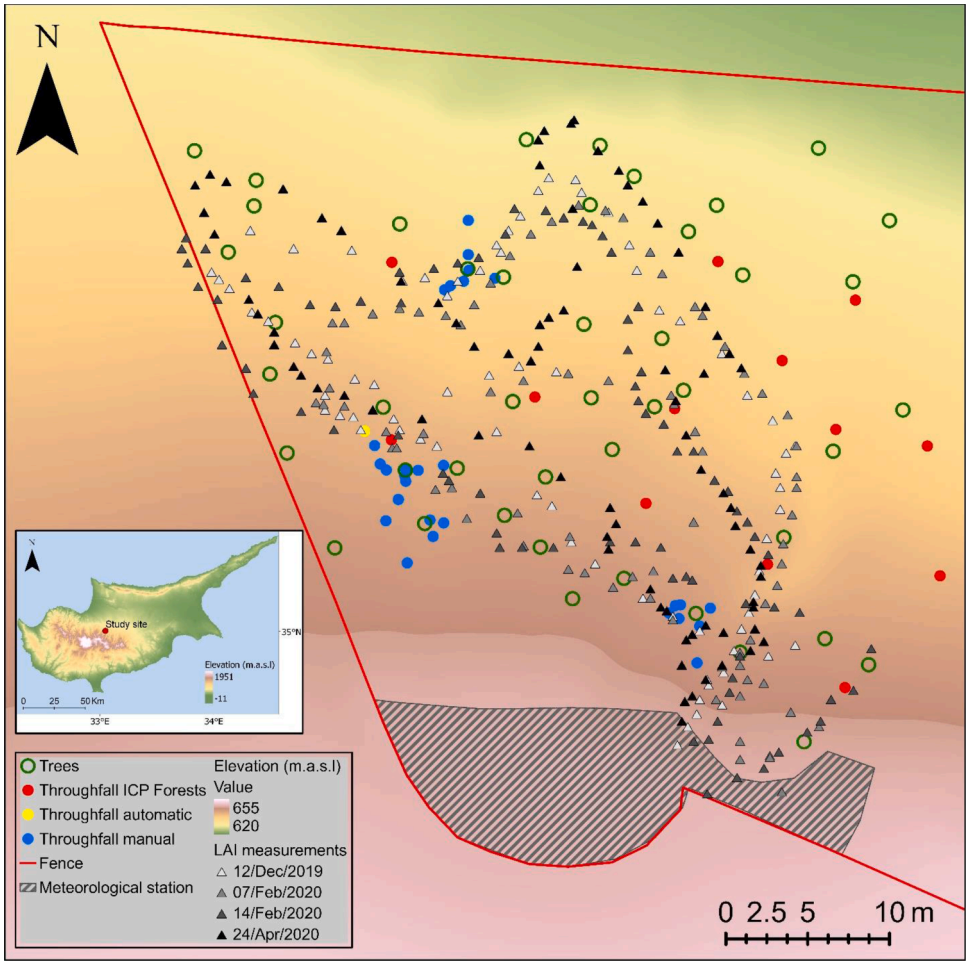

Fig. 1. Map of the study site with the location of the Leaf Area Index (LAI) measurements at four different dates, the location of the trees and the manual, automatic and ICP Forests (International Co-operative Programme on Assessment and Monitoring of Air Pollution Effects on Forests) throughfall gauges.

monitoring network of the International Co-operative Programme on Assessment and Monitoring of Air Pollution Effects on Forests (ICP Forests). The study site is homogenous regarding tree species and stand type and representative of the most important forest species of Cyprus (Department of Forests of Cyprus, 2006; Eliades et al., 2018b; Ferretti et al., 2010). The area is located in a water-limited environment and has a strongly sloping topography with very shallow soils and fractured bedrock (see Table 1). On average, 53% of the rain falls between December and February, while 4% falls between July and September (Camera et al., 2014).

2.1.2. Meteorological data

Meteorological data were provided by the Cyprus Department of Forests from an automatic meteorological station, which is currently maintained by the Cyprus Department of Meteorology. The station is located in an open area at the higher end of the study site (Fig. 1 and 2). Rainfall is measured with a tipping bucket rain gauge (15,189, Lambrecht, Germany) with 0.1 mm/tip resolution, at a height of 1 m above the ground surface. Air temperature and relative air humidity are measured at a height of 2 m (DMA672, LSI Lastem, Italy). Solar radiation is measured by a pyranometer (W m^{-2}) (DPA153, LSI Lastem, Italy), at a height of 2 m, and wind speed is measured with a three-cup anemometer at a height of 10 m (LSI Lastem, Italy). The sensors are connected to a data logger, which records the data at 10-minute intervals. We acquired daily meteorological data for the period from 01/Jan/2008 to 14/Nov/2014 and hourly meteorological data for the period from 15/Nov/2014 to 31/May/2020. Three manual rain gauges (CM1016, ClimeMET, UK) were placed inside the meteorological station on 26/Oct/2017. These gauges were generally measured between one or three days after rainfall and were used to check for missing data in the record of the automatic rain gauge (see Section 2.2.1). Evaporation from these rain gauges is limited by the close fit of the funnel on the receiver.

2.1.3. Throughfall

An automatic rain gauge (model 7857, Davis instruments, USA) with a funnel diameter of 16.5 cm and resolution of 0.2 mm/tip was installed under the tree canopy on 13/Jul/2016. (Fig. 2). Throughfall was recorded with a 5-minute interval with a netDL 500 data logger (OTT HydroMet, Germany). Throughfall was also measured with 28 manual rain gauges (CM1016, ClimeMET, UK), with a collector diameter of 10 cm, which were placed randomly under the canopies of four trees (Fig. 2). These gauges were measured after each rainfall event. In addition, weekly throughfall data for the period between 01/Jan/2008 and 26/Dec/2019, from 15 other manual gauges with an 18-cm diameter, maintained by the Department of Forest of Cyprus for the ICP Forests programme were used for the analysis. The selection of the locations of the ICP Forests throughfall collectors was made using a combination of systematic and random distribution (Clarke et al., 2016). According to this combined approach, the plot area is divided in quadrates of equal sizes and within each quadrate, the sample points are chosen randomly. A summary of the rain and throughfall measurements is presented in Table 2. Stemflow was measured with a flexible PVC tube, which was attached with silicon glue around the trunk of four selected trees at 1.6-m height. The upper part of the tube was cut off to create an open surface and capture the stemflow. The tube was connected to a manual rain gauge. Stemflow, observed between 14/Nov/2014 and 31/Dec/2016, was less than 1% of the total rainfall (M. Eliades et al., 2018). Therefore, we excluded stemflow from the interception model applications.

Table 1
Characteristics of the Agia-Marina-Xyliatou forestry study site; the average annual reference evapotranspiration (ET_o) and rainfall and the minimum and maximum values of rainfall and temperature for the period 1980 – 2010.

Elevation (m)	620 −655
Mean slope (degrees)	25
Aspect	North
Forest density (trees ha^{-1})	200
Tree species	*Pinus brutia*
Average tree height (m)	16
Average tree age (years)	80
Average soil depth (cm)	14
Soil texture	Sandy loam
Bedrock	Basaltic, andesitic and diabasic dykes / pillowed screens
Average annual ET_o (mm)	1263
Average annual rainfall (mm)	425
Minimum annual rainfall (mm)	169 (2007/2008)
Maximum annual rainfall (mm)	670 (2001/2002)
Monthly average daily max. temperature (C°)	34 (July)
Monthly average daily min. temperature (C°)	4 (January)

2.1.4. Leaf area index – Gap fraction

Leaf Area Index (*LAI*) and canopy gap fraction (*p*) were measured with a plant canopy analyser (LAI-2200C, Li-Cor Bioscience, Lincoln, NE, USA). We used two LAI-2250 optical sensors, one for the above canopy measurements (*AC*) and one for the below canopy measurements (*BC*) to measure the attenuation of the radiation by the canopies. These sensors project the image of hemispheric view onto five detectors (rings) arranged to measure the brightness at different zenith angles (7°, 23°, 38°, 53°, 68°). The instrument calculates the gap fraction (*p)* as the interception of the blue light (320–490 nm) at the five zenith angles (θ) from the radiation readings (*Rad*) taken above canopy (*AC*) and below the canopy (*BC*). *LAI* was computed from *p(θ)* according to the procedures of LI-COR Inc. (2017) as:

$$LAI = 2\int_0^{\frac{\pi}{2}} -\ln[p(\theta)]\cos(\theta)\sin(\theta)d\theta \quad (1)$$

where *p(θ)* is the gap probability (fraction) at zenith angle θ, computed as the fraction of the radiation measured below and above the canopy (*Rad(BC)/Rad(AC)*).

The plant canopy analyser was used to measure the *LAI* for the potential evapotranspiration computation (see Section 2.2.3). The *AC* sensor was placed in the open area of the meteorological station, and set to automatic logging every 5 s. We placed the *BC* sensor next to the trunk and below the canopy (1.4-m height) of each of the four trees where the throughfall gauges were located. We took four measurements per tree, representing the four azimuthal directions, on 12/Dec/2019, 7/Feb/2020 and 14/Feb/2020 during uniform overcast sky conditions. We masked the two outer rings of the sensor (53°, 68°), to prevent the sensor from seeing the foliage of neighbouring trees, according to the procedures of the LAI-2200C manual (LI-COR Inc., 2017). We used a 90° view cap to prevent the sensor from seeing the trunk of the tree.

The plant canopy analyser was also used to determine the canopy cover fraction ($c = 1\text{-}p$) of the interception models (see Section 2.5.3). The optical sensor was placed over the funnels of the 28 throughfall gauges and the gap fraction *p* was recorded from the attenuation of diffuse sky radiation at an angle of 7° from zenith, similar to Limousin et al. (2008), on 12/Dec/2019, 7/Feb/2020, 14/Feb/2020 and 24/Apr/2020 during uniform overcast sky conditions. On the same dates, we took 76, 74, 76 and 83 additional *p* measurements within the study site, to compute the canopy cover fraction of the entire plot (Fig. 1). We used the 180° view cap to remove the operator from the sensors view, without masking the outer rings. The measurement interval was approximately one *BC* reading every two meters.

2.2. Field data analysis and computation of evapotranspiration

2.2.1. Data quality check

We performed a Shapiro–Wilk test to examine if the throughfall

Fig. 2. Manual throughfall gauges placed around *Pinus brutia* trees (left) and the meteorological station at the Agia-Marina-Xyliatou forestry site (right).

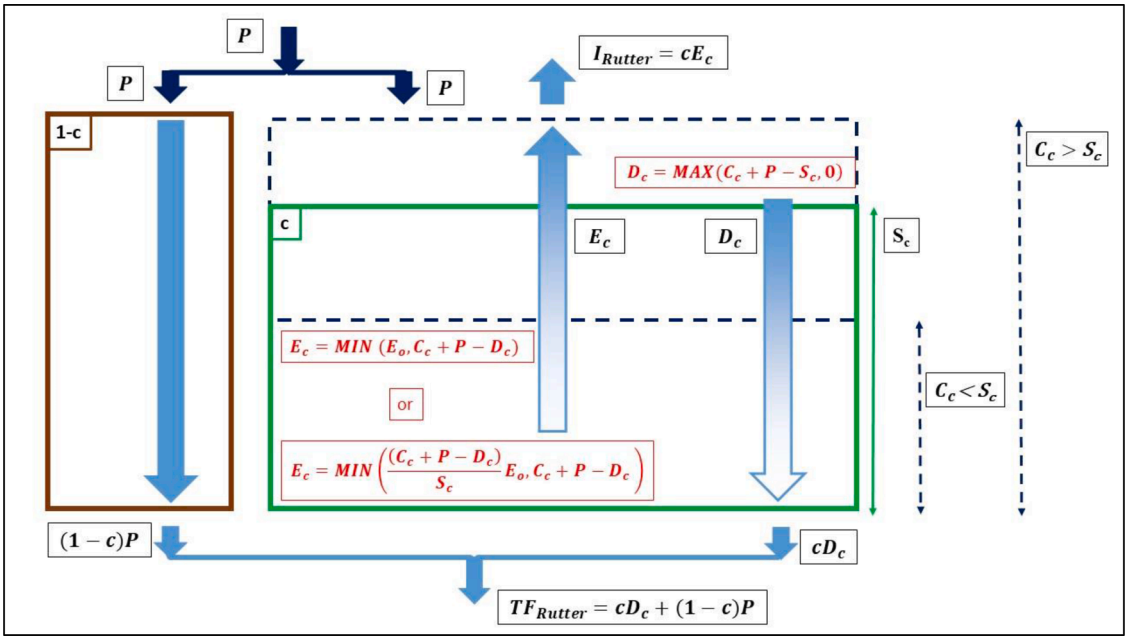

Fig. 3. The conceptual framework of the "sparse" Rutter model (c = canopy cover fraction, 1-c = ground area without canopy cover, P = rainfall, E_o = potential evaporation, C_c = water storage on the canopy surface, S_c = canopy storage capacity, E_c = actual evaporation from the wet canopy cover area, D_c = drainage from the canopy cover area, I_{Rutter} are the modelled interception losses and TF_{Rutter} is the modelled throughfall).

Table 2
Number (N) of meteorological stations, rain gauges (*P*) and throughfall gauges (*TF*), observation periods and measurement intervals.

Observations	N	Period	Interval
Meteorology	1	01/Jan/2008 – 31/May/2020	Daily/Hourly*
P (automatic)	1	01/Jan/2008 – 31/May/2020	Daily/Hourly*
TF (ICP Forests)	15	01/Jan/2008 - 26/Dec/2019	Weekly
P (manual)	3	26/Oct/2017 – 31/May/2020	After rain
TF (manual)	28	14/Nov/2014 – 31/May/2020	After rain
TF (automatic)	1	13/Jul/2016 – 31/May/2020	Hourly (from 5-min)

*Hourly meteorological and rainfall measurements were available from 15 November 2014.

totals of the 28 manual gauges and of the 15 ICP Forests gauges were normally distributed ($\alpha = 0.05$). We subsequently computed the standard error of the mean and the 95% confidence intervals of the throughfall totals of these two data sets, using the t-distribution.

Rainfall data for the periods between 01/May/2017 and 30/Sep/2017 and between 01/Jun/2018 and 21/Jun/2018 were missing because the automatic rain gauge was not working. Due to insufficient power supply there were a few more days with missing hourly rainfall data. Also, due to a failure of the automatic throughfall gauge, no throughfall data were recorded for the period between 04/Dec/2017 and 12/May/2018. In addition, all events for which rainfall occurred at negative temperatures were excluded from the analysis, as ice formed at the funnel opening and blocked the readings. During our frequent field visits to the site, we noted the dates in which pine needles or fallen branches blocked the funnel openings. These events were also excluded.

For all the above missing days, we also removed any following rain days to ensure that we maintained the possible effects of wet canopy on the next day's throughfall. For the days with missing meteorological data, the potential evaporation was estimated from the observations of previous or following hours or days. Thus, we ensured the continuity of rainfall, interception and evaporation of the intercepted rain, before, during and after rainy days. The final record for the period between 01/Jul/2016 and 31/May/2020 contains 1062 days of valid data.

Similar to the hourly data, days with missing potential evaporation data in the long-term dataset (01/Jan/2008 and 26/Dec/2019) were estimated from the observations of previous or following days. We examined the quality of the long-term weekly throughfall data by comparing them with the hourly automated throughfall data for the period from 01/Jul/2016 to 26/Dec/2019. The two throughfall databases showed similar annual throughfall in 2018 and 2019 but large deviations in 2016 and 2017 (Supplementary material, Table S1 – Fig. S2). The data comparison indicated that during these years missing weekly throughfall data may have been recorded as zero. For example, for the week of 07/Sep/2016, the record showed 0 mm throughfall, while we had 12.0 mm rainfall and the throughfall derived from the hourly data was 10.9 mm.

2.2.2. Hourly throughfall

The hourly records from the automatic throughfall gauge were used to partition the event-based throughfall observations from the 28 manual gauges into hourly throughfall. First we examined whether the automatic throughfall collector is representative of the average throughfall of the 28 manual throughfall gauges. This was done with an F-test and a *t*-test on a total of 126 throughfall events. The F-test indicated that the variances of the two populations are equal (p-value = 0.303) and the *t*-test results showed that the means of the two populations are equal (p-value = 0.381). Thus, the mean hourly throughfall ($TF_{mean(i)}$) was computed as:

$$TF_{mean\ (i)} = TF_{auto\ (i)} * \frac{TF_{manual(j)}}{\sum_{i=1}^{n} TF_{auto}(j)} \quad (2)$$

where $TF_{auto(i)}$ is the throughfall measured by the automatic throughfall gauge at hour *i*, $TF_{manual(j)}$ is the average throughfall of the 28 manual gauges measured for event *j* and ΣTF_{auto} is the sum of the automatic throughfall measured for all the hours (*n*) of event *j*. We used the median instead of the average of the 28 manual gauges for 21 of 126 events where we had missing values from one or more of the 28 manual gauges. For the 105 events with no missing data, the mean *TF* of the 28 gauges averaged to11.6 mm and the median *TF* averaged to 11.8 mm.

2.2.3. Evaporation from the wet canopy surface

The potential wet surface evaporation per unit ground area (assuming a uniform "closed" canopy surface) was computed with the Penman-Monteith equation (E_o) with the canopy resistance (r_s) set to zero:

$$E_o = \frac{1}{\lambda} \frac{\Delta\ (R_n) + \frac{p_a c_p D}{r_a}}{\Delta + \gamma} \quad (3)$$

where Δ is the slope of saturation vapour pressure curve (kPa/ °C), R_n the net radiation (MJ/m^2), p_a is the density of dry air (kg m^{-3}), c_p the specific heat of the air (J kg^{-1} °C^{-1}), *D* the vapour pressure deficit (kPa), r_a the bulk aerodynamic resistance between the leaf surfaces and the reference point (2 m above the top of the canopy), λ the latent heat of vaporization of water (MJ/kg) and γ is the psychometric constant (kPa/ °C). The net radiation was computed according to the procedures of Allen et al. (1998). The aerodynamic resistance (r_a) was computed as follows (Monteith, 1965):

$$r_a = \frac{\ln\left\{\frac{(z-d)}{z_0}\right\}^2}{k^2 u} \quad (4)$$

where *k* is von Karman's constant (0.41), *u* (m s^{-1}) is the wind speed at height *z* (m), *z* is the reference height (m), *d* is the zero plane displacement height (m), and z_0 is the roughness length of the canopy (m). The reference height was 2 m above the top of the tree canopy.

The parameters *z*, *d* and z_0 were computed according to the procedures of Shuttleworth and Gurney (1990). The z_0 was computed as:

$$z_0 = 0.3(h_c - d) \quad (5)$$

where h_c is the average tree height (m), measured with an analogue height metre (h_c is 16 m). The zero plane displacement *(d)* was computed as:

$$d = 1.1 h_c \ln\left\{1 + (C_d LAI)^{0.25}\right\} \quad (6)$$

where *LAI* is the leaf area index (m^2/m^2) and C_d is the mean drag coefficient for individual leaves. The drag coefficient was computed as:

$$C_d = \frac{\left[-1 + exp\left(0.909 - \frac{3.03 z_c}{h_c}\right)\right]^4}{4} \quad (7)$$

where z_c is the roughness length for a closed canopy (m), defined as $0.05h_c$.

2.3. Model descriptions

We used the revised versions of Rutter, Gash and Liu models to compute interception losses. In the revised versions of these models the canopy cover fraction (*c*) is assumed to be equal to one minus the gap fraction (*1-p*). The Rutter model is applied both on an hourly and daily basis. The Gash and Liu models were originally developed for the computation of interception losses on an event basis (Gash, 1979; Liu, 2001). A time interval that will allow the canopy to dry completely after rainfall ceased should be used to separate the different rainfall events. However, we applied both models on a daily basis with the assumption that the canopy is dry at the start of each day (Gash, 1979; Liu, 2001). As noted in Section 2.1.3, because of the small fraction of stem flow observed in the study site (less than 1%), we did not explicitly model stem flow, thereby assuming that the trunks behave as an integral part of the canopy.

2.3.1. Revised Rutter model

We applied the revised ("sparse") version of the Rutter rainfall interception model (Rutter et al., 1971), formulated by Valente et al. (1997). The Rutter model is a single-layer model, following the assumption that evaporation is one dimensional with no horizontal interactions (Rutter et al., 1971; Valente et al., 1997).

We applied the simplified drainage function where any excess water above the canopy storage capacity is converted immediately into drainage and canopy drainage stops when the rainfall ceases (Valente et al., 1997). We used the hourly totals of *P* and E_o for the hourly model and the daily sums of the hourly totals for the daily model. For each time step (hour or day), the water balance of the canopy-covered area (*c*) is calculated as follows (Fig. 4):

$$C_c(t) = C_c(t-1) + P(t) - D_c(t) - E_c(t) \quad (8)$$

where $C_c(t)$ and C_c *(t-1)* are the water storages on the canopy covered area (mm) at time *t* and time *t-1*, respectively, *P(t)* is the rainfall (mm) during time step *t*, $D_c(t)$ is the canopy drainage from the canopy covered area (mm) during time step *t*, and $E_c(t)$ is the actual evaporation from the wet canopy covered area (mm) during time step *t*,

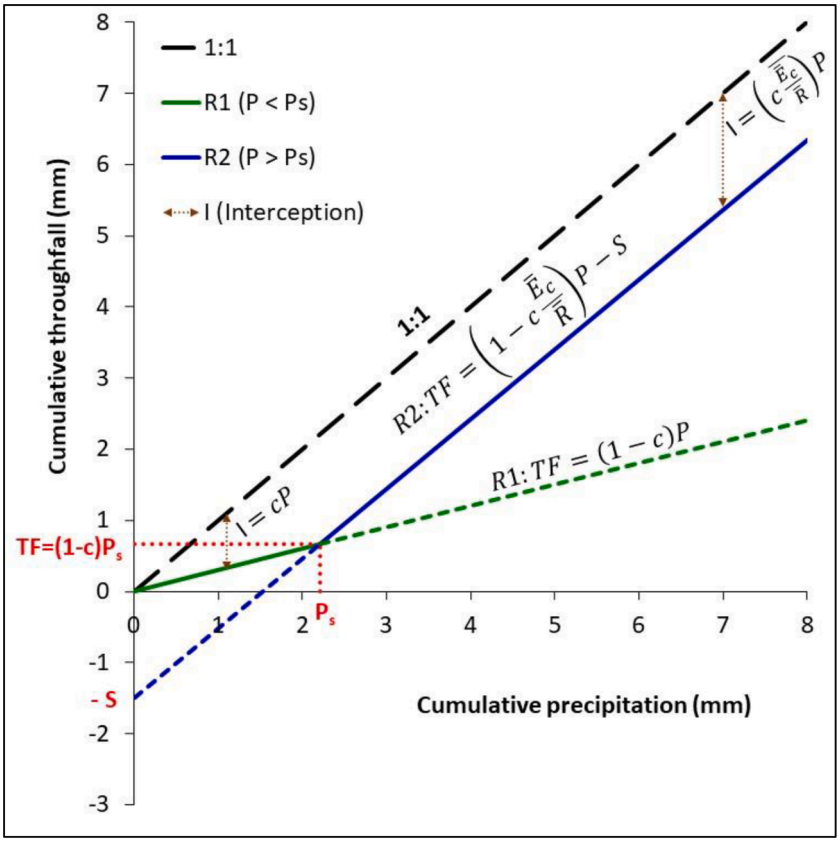

Fig. 4. The regression lines for rainfall events that do not fill (*R1*) and fill (*R2*) the canopy storage capacity (modified from Licata et al., 2011). At the crossing of the two lines *P* is equal to P_s and *TF* is equal to *(1-c)*P_s. The slope of the *R1* line is equal to *1 - c* and the negative intercept of the *R2* line is equal to the canopy storage capacity (*S*).

Drainage is computed as:

$$D_c(t) = MAX(C_c(t-1) + P(t) - S_c, 0) \tag{9}$$

where S_c is the canopy storage capacity per unit area of cover (*S/c*) (mm), *S* is the canopy storage capacity per unit ground area (mm) and *c* is the canopy cover fraction. E_c is computed as:

$$E_c(t) = MIN\left(\frac{(C_c(t-1) + P(t) - D_c(t))}{S_c} E_o(t),\ C_c(t-1) + P(t) - D_c\ (t)\right) \tag{10}$$

where $E_o(t)$ is the potential evaporation as computed with the Penman-Monteith equation (Eq. (3)).during time step *t* The fraction in front of E_o is the relative depth of the water storage on the canopy area (canopy wetness), which takes values between 0 and 1. Multiplication of E_c with *c* yields the canopy evaporation per unit ground area. The interception (I_{Rutter} *(t)*) and throughfall (TF_{Rutter} *(t)*) over the ground area during time step *t* are computed as:

$$\mathrm{I_{Rutter}}\ (t) = c\mathrm{E_c}(t) \tag{11}$$

$$\mathrm{TF_{Rutter}}(t) = c\mathrm{D_c}(t) + (1-c)\mathrm{P}(t) \tag{12}$$

Van Dijk et al. (2015) questioned the validity of (Eq. (10)) because it would prevent the canopy from ever drying completely. Thus, if we assume, similarly to Van Dijk et al. (2015), that evaporation from the canopy is not a function of the amount of water on the canopy, E_c can also be computed as:

$$\mathrm{E_c}(t) = \mathrm{MIN}(\mathrm{E_o}(t),\ \mathrm{C_c}(t-1) + P(t) - \mathrm{D_c}(t)) \tag{13}$$

We found small differences in the interception losses (0 - 2.9%) between the two assumptions (Eq. (10) and Eq. (13)) for 400 different combinations of *S* and *c* (Supplementary material, Fig. S3). We applied (Eq. (13)) in the analysis henceforward.

Note that in the above equations, during each time step, we first subtract the drainage and then the evaporation. If we would first subtract the evaporation and then the drainage, throughfall would be less than 0.5% lower for the hourly model and 11.0% lower for the daily model, when using the S and c optimized with the above equations (Supplementary material, Table S2).

2.3.2. *Revised Gash model*

The second model used in this study was the revised version of the Gash rainfall interception model (Gash et al., 1995). According to the model formulation there is no dripping (throughfall) from a partially wetted canopy and the canopy becomes saturated after rainfall exceeds the critical amount of rain (P_s). The interception loss by the Gash model (I_{Gash}) is computed as:

$$I_{Gash} = c\sum_{j=1}^{m} P_j + c(nP_s) + c\frac{\overline{E_c}}{\overline{R}}\sum_{i=1}^{n}(P_i - P_s) \tag{14}$$

where P_j is the rainfall during *m* events with insufficient rain to saturate the canopy ($P < P_s$) (mm/event), P_s is the amount of water needed to saturate the canopy (mm), P_i is the rainfall during *n* events that saturate the canopy ($P \geq P_s$) (mm/event), $\bar{R}$ and $\bar{E}_c$ are, respectively, the mean rainfall rate (mm h^{-1}) and mean evaporation rate from the wet canopy (mm h^{-1}) under saturated canopy conditions. All rainfall parameters are expressed, in the usual manner, over the ground area.

The Gash model follows the same assumption as Rutter et al. (1971), i.e., evaporation during the wetting phase is linearly proportional to the water storage on the canopy (Eq. (10)). Assuming a constant rainfall rate and no drainage before saturation, Gash (1979) derived the following

analytical solution for the amount of water needed to saturate the canopy:

$$P_s = -\frac{\bar{R}}{\bar{E}_c}\left(\frac{S}{c}\right)\ln\left(1-\frac{\bar{E}_c}{\bar{R}}\right) \quad (15)$$

Klaassen et al. (1998) noted that interception equations can be simplified, if we assume that evaporation is represented by a constant ratio between $\bar{E}$ and $\bar{R}$ during rain, instead of as a function of the canopy water storage during wetting. He found minimal differences in S for the two approaches ($S = 1.0$ mm for the first, $S = 1.06$ mm for the last), for $\bar{E}/\bar{R} = 0.1$. Thus, if we assume that canopy evaporation during the wetting phase is not a function of the depth of the water storage on the canopy, evaporation before and after canopy saturation will be the same ($E = c\,\bar{E}_c/\bar{R} \times P$) and we obtain the following equation for P_s:

$$P_s = \frac{S}{c\left(1-\frac{\bar{E}_c}{\bar{R}}\right)} \quad (16)$$

The derivation of this equation is shown in Section 2.5.2. Eq. (16) makes the conceptualization of interception similar to that of the Rutter model with Eq.13. We found minor differences (less than 0.5%) in the computed interception between the two different equations (Eq.15 and Eq.16) (Supplementary material, Fig. S3). Hereafter, we used Eq. (16) for the analysis. A similar P_s assessment was made by Návar (2020) by breaking the I vs. P relationship to independently derive the rate of canopy wetting and the rate of evaporation during a storm.

2.3.3. Revised Liu interception model

The third model used in this study is the Liu interception model (Liu, 1997). The model assumes that the canopy water storage increases exponentially (wetting process) until canopy storage capacity is reached, while drainage occurs even before reaching the canopy storage capacity (Liu, 2001, 1997). In the derivation of the model, the measure of the saturation of the canopy storage ($1 - C/S$), is described as the canopy dryness index (DI). Assuming that the canopy at the beginning of each rainfall event is dry ($DI = 1$ or $C = 0$), rainfall interception (I_{Liu}) during a single storm can be computed as:

$$I_{Liu} = S\left[1-exp\left(-\frac{(1-p)}{S}P\right)\right]\left[1-\frac{\bar{E}}{(1-p)\bar{R}}\right]+\frac{\bar{E}}{\bar{R}}P \quad (17)$$

where P is the amount of rainfall during a storm event (mm/event). Carlyle-Moses and Price (2007) corrected the original Liu model as:

$$I_{Liu} = S\left[1-exp\left(-\frac{c}{S}P\right)\right]\left[1-\frac{\bar{E}_c}{\bar{R}}\right]+c\,\frac{\bar{E}_c}{\bar{R}}P \quad (18)$$

Liu (2001, 1997) extracted the parameters c, S, $\bar{E}$ and $\bar{R}$ from the literature to evaluate the model.

2.4. Sensitivity analysis

We examined the sensitivity of the models to S, c and $\bar{E}_c/\bar{R}$ (Gash and Liu) or E_o (Rutter). The initial parameter values were set to 2 mm for S, 0.5 for c and 0.02 for $\bar{E}_c/\bar{R}$. For the Rutter model, we used the E_o time series computed from the meteorological observations as initial value. We changed the initial value of each parameter by ± 80%, using 20% intervals, while we kept the other parameters at their initial values. We computed the relative sensitivity (RS) as:

$$RS = dI \Big/ dJ = \frac{I_{test}-I_{initial}}{I_{initial}} \Big/ \frac{J_{test}-J_{initial}}{J_{initial}} \quad (19)$$

where dI is the relative change in the computed interception and dJ is the relative change in the input parameter, $I_{initial}$ is the interception loss (% of P) for the initial value of the input parameter ($J_{initial}$) and I_{test} is the interception loss (% of P) for a selected input test parameter value (J_{test}).

We examined the equifinality of the Rutter, Gash and Liu models through 400 test runs with different combinations of the parameters S and c. The range of tested storage capacity (S) values was from 0.1 to 4.0 mm with a 0.1 mm interval. The range of the canopy covered fraction (c) values was from 0.1 to 1 with a 0.1 interval. We used the computed $\bar{E}_c/\bar{R}$ value for the Gash and Liu models, with $\bar{R}_{sat}$ set to 0.5 mm h^{-1} (see Section 2.5.1) and E_o from the observations for the Rutter model. We conducted another 400 test runs with different combinations of the parameters S and $\bar{E}_c/\bar{R}$ to examine the equifinality of the Gash and Liu models under the conditions of an open forest ($c = 0.7$). The S values were the same as above and the range of the $\bar{E}_c/\bar{R}$ values was from 0.01 to 0.19 with a 0.02 interval. The rainfall and evaporation data for the period between 01/Jul/2016 and 31/May/2020 were used for the sensitivity and equifinality analyses.

2.5. Model assumptions and parameter derivation procedures

The ratio of the mean evaporation rate to the mean rainfall rate ($\bar{E}_c/\bar{R}$) can be computed from hourly E_o and P observations (Section 2.5.1) or from the regression method (Section 2.5.2). The parameters S and c are also derived with this method. Alternatively, the parameters S and c can be derived with optimization, as described in Section 2.5.3.

2.5.1. Rainfall rate threshold

Gash (1979) assumed that after canopy saturation, a rainfall rate threshold ($\bar{R}_{sat}$) of 0.5 mm h^{-1} is needed to maintain saturated canopy conditions. Under this assumption, hourly values of E_o and P can be averaged for all hours with $P > 0.5$ mm h^{-1}, to estimate $\bar{E}_c$ and $\bar{R}$ for saturated canopy conditions. We tested a range of rainfall rate thresholds, from 0.1 to 1.4 mm h^{-1}, with a 0.1 mm h^{-1} interval and examined the effect of differences in $\bar{E}_c$, $\bar{R}$ and their ratio on interception. The $\bar{R}$ and $\bar{E}_c$ values were computed as the mean of the hourly P and E_o values, respectively, for the hours where P exceeds the rainfall rate threshold. The rainfall and evaporation data for the period between 01/Jul/2016 and 31/May/2020 were used to test the different rainfall rate thresholds.

2.5.2. Regression method

Regression-based methods from the scatter plots of TF versus P are often used to extract the model parameters. According to Klaassen et al. (1998), the scatter plot of TF versus P can be divided into a wetting part and a saturated part. This method relies on the least square fitting of data and is generally referred to as the mean method. Two linear regression lines between throughfall and rainfall are plotted for rainfall events that do not (R1: $P < P_s$) and do (R2: $P > P_s$) saturate the canopy, as illustrated in Fig. 4. Before canopy saturation ($P < P_s$), interception losses consist of canopy storage filling and evaporation, whereas throughfall consists of the rain that falls through the canopy cover. Thus, R1 is given by:

$$TF = (1-c)P \quad (20)$$

And interception is the complement of the throughfall:

$$I = cP \quad (21)$$

After saturation ($P > P_s$), interception losses consist of evaporation only. Because evaporation is assumed to be the same over the full rainfall event (i.e., not a function of saturation), the total interception for rainfall events ($P > P_s$) is given by:

$$I = \left(c\,\frac{\bar{E}_c}{\bar{R}}\right)P + S \quad (22)$$

Thus, throughfall, specified by R2, is equal to:

$$TF = \left(1-c\,\frac{\bar{E}_c}{\bar{R}}\right)P - S \quad (23)$$

At the crossing of the two lines P is equal to P_s and we can derive P_s as

follows:

$$(1-c)P_s = \left(1 - c\,\frac{\overline{E_c}}{\overline{R}}\right)P_s - S \rightarrow P_s = \frac{S}{c\left(1-\frac{\overline{E_c}}{\overline{R}}\right)} \quad (24)$$

The P_s equation is the same as presented in Eq. (16). The two regression lines can be determined by data fitting (e.g., least square fitting) of rainfall and throughfall observations, using several iterations with different values of P_s. Obviously, the derivation of the model parameter values with the regression method implies that evaporation before canopy saturation is not a function of the depth of water on the canopy. In contrast to the approach by Jackson (1975), who assumed that evaporation is negligible during the storm, we assume a constant evaporation rate during the entire rainfall event.

We used the daily *TF* and *P* data from 01/Jul/2016 to 31/Dec/2018 to derive the model *c, S* and $\bar{E}_c/\bar{R}$. We tested a range of P_s values (0.5 – 4 mm) with a trial and error approach, where we selected the P_s value that resulted in the average highest correlation (r^2) of the two regression lines. We also tested the effect of the different rainfall event separation intervals (2 h, 6 h and 12 h) on the derivation of the model parameters *S, c* and $\bar{E}_c/\bar{R}$.

2.5.3. Automatic model parameterization

We calibrated the Rutter, Gash and Liu models with the use of an automatic model parameterization procedure: (i) for the derivation of *S* and *c* (optimization-*S,c*) and (ii) for the derivation of *S* with *c* set equal to the value measured with the plant canopy analyser (optimization-*S*) (Table 3). We used the computed $\bar{E}_c$ and $\bar{R}$ values for the Gash and Liu models, with $\bar{R}_{sat}$ set to 0.5 mm h^{-1} (see Section 2.5.1). The Microsoft Excel Solver, set to nonlinear programming with the generalized reduced gradient method (Fylstra et al., 1998) was used for the optimization. The optimal parameter value set for each model was selected based on the highest Kling-Gupta efficiency (*KGE)*, with a constraint of ±10% for the percent bias (*P.BIAS*). The *P.BIAS* and *KGE* were computed as:

$$P.BIAS = \frac{\sum_{i=1}^{n}(\widehat{TF}_i - TF_i)}{\sum_{i=1}^{n}(TF_i)} \quad (25)$$

$$KGE = 1 - \sqrt{(r-1)^2 + (\alpha-1)^2 + (\beta-1)^2} \quad (26)$$

where *n* is the number of observations, $\widehat{TF}_i$ and *TFi* are the simulated and observed throughfalls (mm) for the time interval *i* (hourly or daily), respectively, *r* is the correlation coefficient between simulated and observed throughfall, α is the ratio between the means of the simulated and observed throughfall (bias ratio), and β is the ratio between the standard deviations of the simulated and observed throughfall. We also computed the sum of the absolute daily errors (*SAE*). These same model evaluation indices were also used to evaluate the performance of the regression method.

We calibrated the models with the two above-mentioned automatic parameterization methods for the period between 01/Jul/2016 and 31/Dec/2018 (571 days) and then validated them for the period between 01/Jan/2019 and 31/May/2020 (491 days). To make the model evaluation comparable, the performance criteria for the hourly Rutter model were computed on the daily totals.

Table 3
The model input parameters (*P* = rainfall, E_o = evaporation, $\bar{R}$ = mean rainfall rate, $\bar{E}_c$ = mean evaporation rate, P_s = amount of water needed to saturate the canopy, *S* = storage capacity, *c* = canopy cover fraction) and their derivation procedures.

Input Parameter	Parameter derivation method	Models
P (mm)	Measured (Section 2.1.2)	Rutter, Gash, Liu
E_o (mm)	Computed (Section 2.2.3)	Rutter
$\bar{R}$ (mm h^{-1})	Computed (Section 2.5.3)	Gash, Liu
$\bar{E}_c$ (mm h^{-1})	Computed (Section 2.5.3)	Gash, Liu
S (mm)	*Optimization-S,c, Optimization-S*	Rutter, Gash, Liu
c	*Optimization-S,c* / measured (Section 2.1.4)	Rutter, Gash, Liu
P_s (mm)	(Eq. (16))	Gash

2.6. Long-term model application (2008 – 2019)

We used the derived parameter values of *S, c* and $\bar{E}_c/\bar{R}$ from the two automatic model parameterizations and from the regression method for the long-term model application. We examined the differences between the annual sums of the simulated daily throughfall of the daily Rutter, Gash and Liu models and the long-term weekly throughfall data, for the 12 year period from 01/Jan/2008 to 26/Dec/2019.

3. Results

3.1. Meteorological data, throughfall and canopy characteristics

The Shapiro-Wilk test showed that the throughfall totals of the 28 manual gauges (p-value = 0.099) and of the 15 ICP Forests (p-value = 0.365) gauges were normally distributed. The total rainfall for the period from 01/Jul/2016 to 31/May/2020 was 2173.8 mm and the average throughfall from the 28 manual gauges was 1716.0 mm (79% of *P*). The standard error of the mean *TF* was 61.1 mm and the 95% confidence interval was 1716.0 ± 117.6 mm. This is equivalent to a margin of error of ±7%. This falls within the error range (5 – 10%) that was reported in previous studies (Holwerda et al., 2006a; Kimmins, 1973; Rodrigo and Àvila, 2001). Similarly, rainfall and average throughfall of the 15 ICP Forests gauges for the period from 01/Jan/2008 to 26/Dec/2019 were 5147.8 and 3814.3 mm (74% of *P*), respectively. The standard error of the mean *TF* was 222.4 mm and the 95% confidence interval was 3814.3 ± 435.9 mm. This gives an error of ±11.4%, showing the larger uncertainty of this data set.

Daily rainfall for the 2016 - 2020 observations is shown in Fig 5. After the exclusion of the days with missing data (see Section 2.2.1), rainfall was 667.8 mm during the period from 01/Jul/2016 to 31/Dec/2018 (Calibration period) and 837.6 mm during the period from 01/Jan/2019 to 31/May/2020 (Validation period). The number of rain days between 01/Jul/2016 and 31/Dec/2018 was 110 out of a total of 571 days, while there were 118 rain days out of 491 days between 01/Jan/2019 and 31/May/2020. The number of rain days with less than 2 mm rain ($P_{<2}$) for the calibration period was 52 and amounted to 4.6% of the total rainfall, while for the validation period the number of $P_{<2}$ days was 45 and amounted to 3.2% of the total rainfall. The number of $P_{<2}$ days for the 2008 – 2019 period was 409 (from a total of 910 rain days) and amounted to 5.5% of the total rainfall (Supplementary material, Fig. S5).

The number of hours with rainfall intensities between 0.1 and 0.5 mm h^{-1} was 45% of the total number of hours with rain (1055), but the sum of the rainfall for these intensities was only 6% of the total of 1505 mm (Fig. 6). The highest hourly rain was 45.0 mm h^{-1} on 31/May/2018 and 30.0 mm h^{-1} on 03/April/2019 (Fig. 6). On 31/May/2018 we had also the highest daily rainfall of 70.7 mm. The highest consecutive rainfall was 37 h (83.1 mm), recorded between 14/Jan/2019 18:00 and 16/Jan/2019 05:00.

The average *LAI*, measured with the plant canopy analyser, for the four *Pinus brutia* trees was 2.38, ranging from 2.19 (12/Dec/2019) to 2.60 (7/Feb/2020). The average canopy cover fraction (*c*) over the funnels of the 28 throughfall gauges was 0.69, ranging from 0.24 to 0.93 (Supplementary material, Fig. S4). The *c* measured over the 28 throughfall gauges was representative for the entire study area where the average, measured canopy cover fraction was 0.70.

The average daily E_o for the wet days was 2.3 mm during the calibration period and 2.0 mm during the validation period. Similarly, the average daily E_o for the dry days was 4.2 mm during the calibration period and 4.5 mm during the validation period.

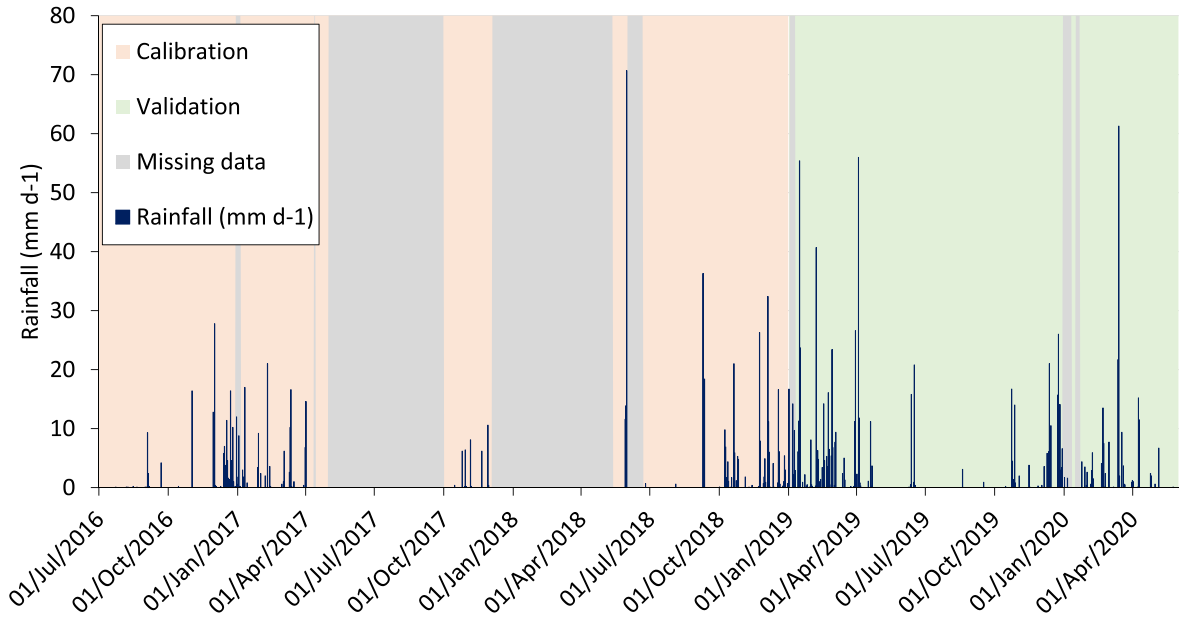

Fig. 5. Daily rainfall (mm d^{-1}) for the period between 01/Jul/2016 and 31/May/2020.

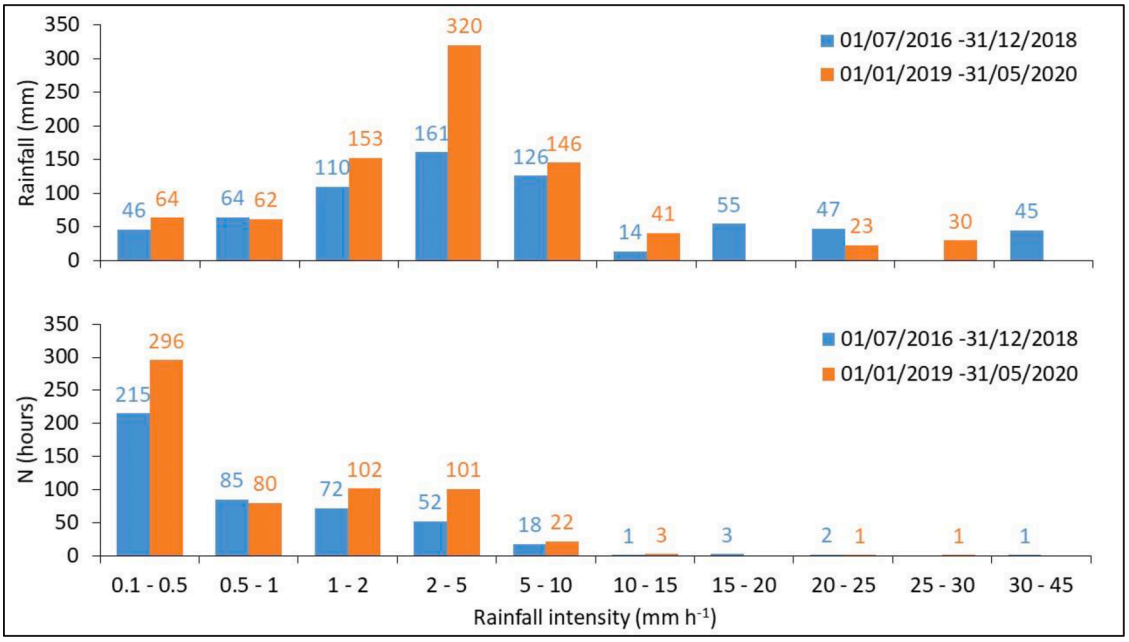

Fig. 6. Rainfall amount (mm)(upper) and number of rainfall hours (N) (lower) for each rainfall intensity class. Blue bars denote the calibration period (01/Jul/2016 – 31/Dec/2018) and orange bars denote the validation period (01/Jan/2019 – 31/May/2020).

3.2. Sensitivity analysis

The results of the sensitivity analysis of the computed interception to changes of S, c and $\bar{E}_c/\bar{R}$ or E_o for the 01/Jul/2016 and 31/May/2020 period are shown in Fig. 7. The relative sensitivity of the Rutter model to E_o (−47% to 18% changes in interception for ±80% change in E_o) was much higher than the relative sensitivity of the Gash and Liu models to $\bar{E}_c/\bar{R}$ (−4% to 4% changes in interception for ±80% change in $\bar{E}_c/\bar{R}$). The evaporation values in all three models were derived from the hourly observations. However, the Gash and Liu model use a constant $\bar{E}_c/\bar{R}$ throughout the model application period, whereas the Rutter model uses the actual observations (plus or minus the relative change for the sensitivity analysis).

The changes in S within $a \pm 80\%$ range showed that the Gash model was the most sensitive to S (−68% to 43% change in interception losses) and the hourly Rutter model the least sensitive (−57% to 33%). Conversely, for changes in c within $a \pm 80\%$ range, the highest relative change in interception loss was found for the hourly Rutter model (–61% to 33%), and the smallest for the Gash model (−56% to −19%).

The results of the different combinations of the parameters S and c, on the computed interception losses by the Rutter, Gash and Liu models are presented in Fig. 8. All models show equifinality, meaning that a range of combinations of the input parameters S and c will result in the same interception loss. Equifinality is especially strong at an interception of 9% of P which within our set-up can be obtained by 20 combinations of S and c with the Rutter model (both hourly and daily), 32 combinations with the Gash model and 12 combinations with Liu model. Interception losses, obtained with a complete canopy cover ($c = 1$) and

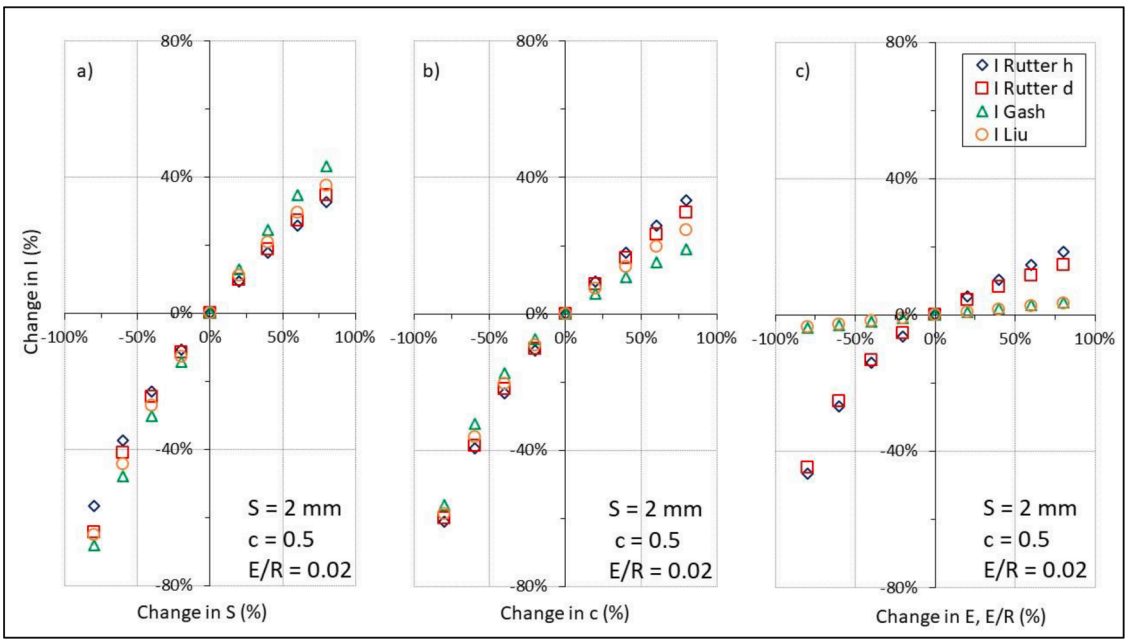

Fig. 7. The relative change in interception loss (I) of the hourly (h) and daily (d) Rutter model, Gash and Liu models resulting from relative changes in S (a), c (b) and $\bar{E}_c/\bar{R}$ and Eo for Rutter (c), from their initial values as shown in the graph.

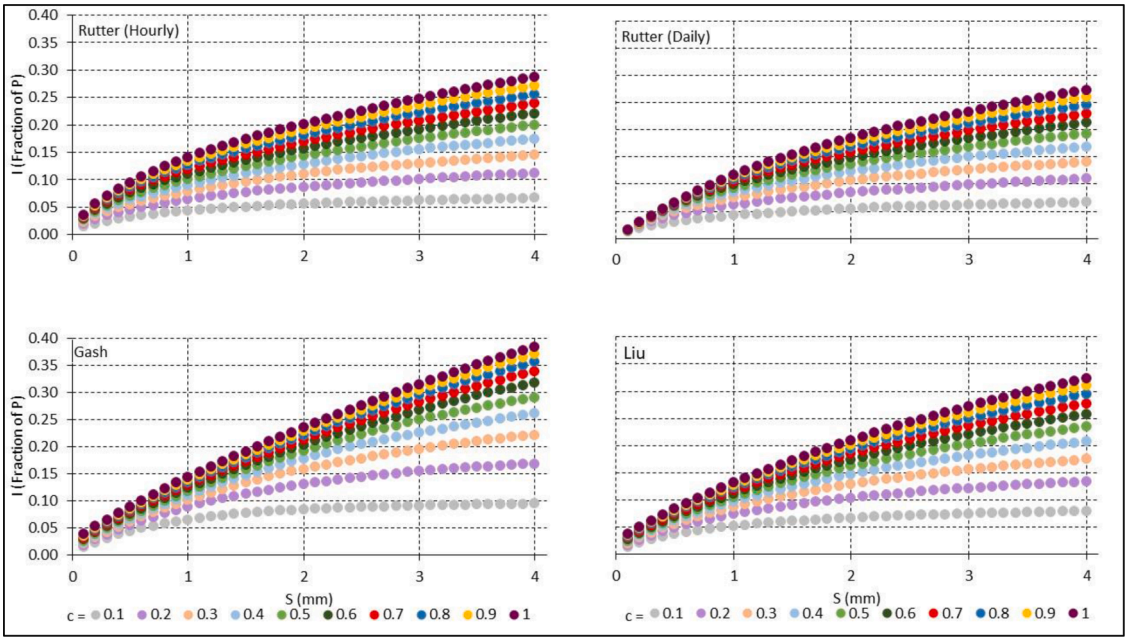

Fig. 8. The interception loss as a fraction of rainfall (I/P) of the hourly Rutter and of the daily Rutter, Gash and Liu models (01/Jul/2016 - 31/May/2020) with changing canopy cover fraction (c) and storage capacity (S).

canopy storage (S) of 2 mm, amount to 20%, 19%, 24% and 21% of P for the hourly Rutter and daily Rutter, Gash and Liu models, respectively. These modelled interception losses would increase to values of 28%, 27%, 38% and 32% of P, respectively, for a canopy storage of 4 mm, which is, however, an unlikely high value for a semi-arid Mediterranean forest. Thus, the higher sensitivity to changes S of the Gash model, compared to the other three models, results in the highest modelled interception losses (38%) with a full canopy cover.

The Gash and Liu models show also equifinality for different combinations of the parameters S and $\bar{E}_c/\bar{R}$ (Fig. 9). A rainfall interception of 18% of P is modelled with 10 S-$\bar{E}_c/\bar{R}$ combinations by the Gash model and with 15 S-$\bar{E}_c/\bar{R}$ combinations by the Liu model.

3.3. Model assumptions and parameter derivation procedures

3.3.1. Rainfall rate threshold

The effect of the different rainfall rate thresholds on the computed $\bar{E}_c$, $\bar{R}$, and $\bar{E}_c/\bar{R}$ for the period between 01/Jul/2016 and 31/May/2020 is presented in Fig. 10. Both $\bar{E}_c$ and $\bar{R}$ decreased with increasing rainfall rate threshold. The $\bar{E}_c$ values ranged from 0.02 mm h^{-1} for $\bar{R}_{sat}$ of 1.4 mm h^{-1} to 0.05 mm h^{-1} for $\bar{R}_{sat}$ of 0.1 mm h^{-1}. The $\bar{R}$ values varied less, ranging from 1.1 to 1.4 mm h^{-1}. The resolution of the rainfall tipping bucket (0.1 mm) adds an uncertainty of ±0.1 mm to the results, because any rainfall less than 0.1 mm will remain on the tipping bucket and will either evaporate or become part of the next rainfall event. The ratio $\bar{E}_c/\bar{R}$

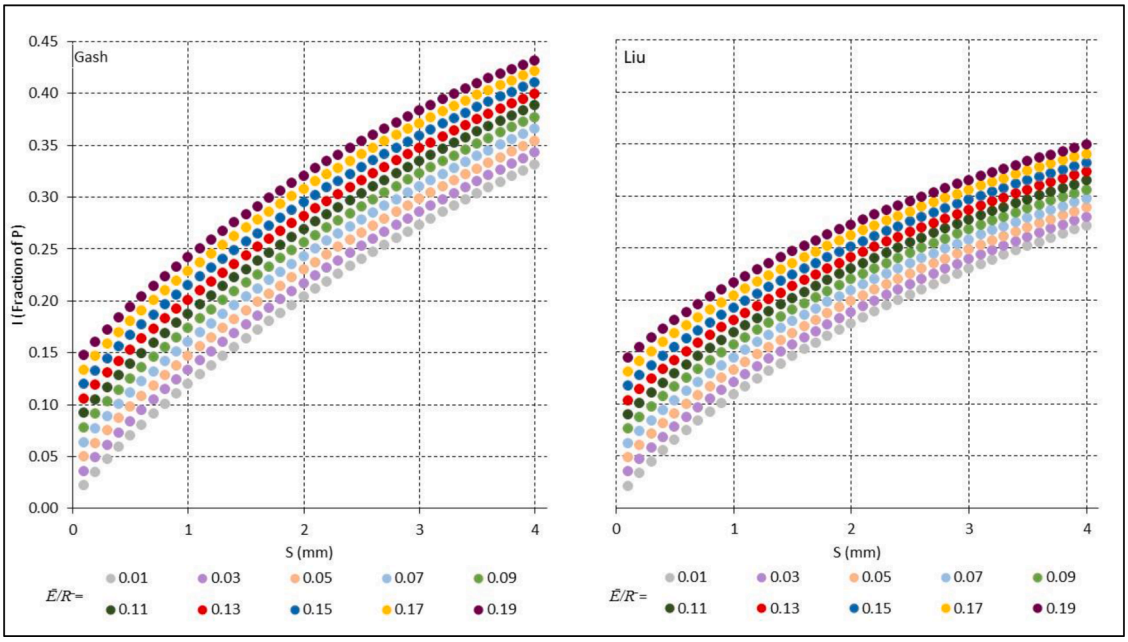

Fig. 9. The interception loss (as a fraction of rainfall) of the Gash and Liu models (01/Jul/2016 - 31/May/2020) with changing canopy storage capacity (S) and mean evaporation to mean rainfall ratio ($\bar{E}_c/\bar{R}$) and c equal to 0.7.

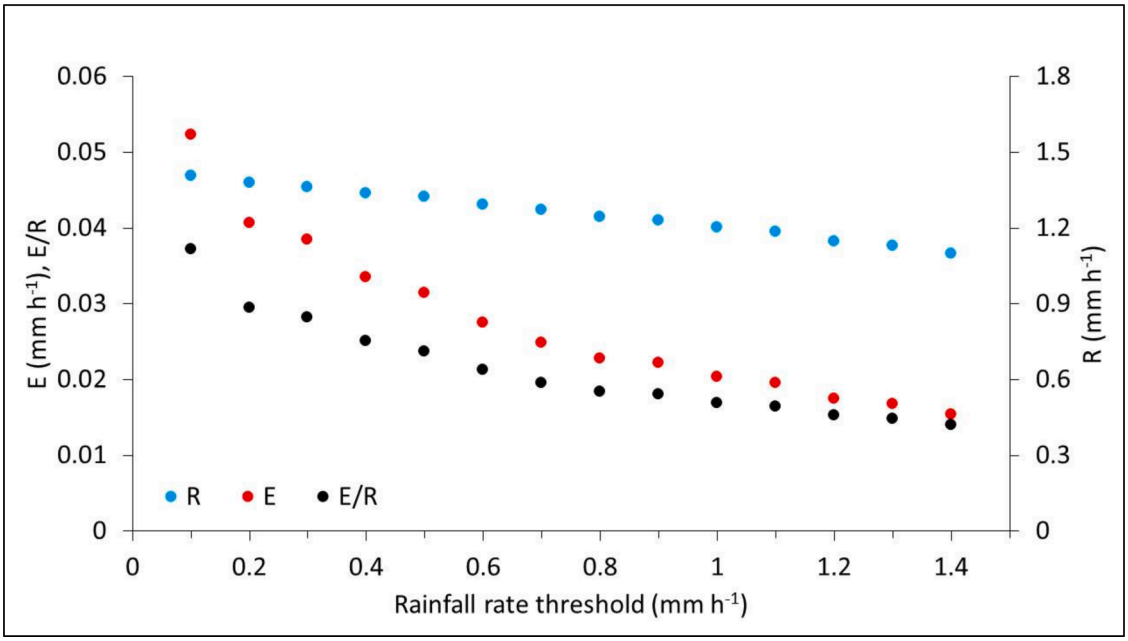

Fig. 10. Change in mean evaporation rate ($\bar{E}_c$), mean rainfall rate ($\bar{R}$), and their ratio ($\bar{E}_c/\bar{R}$) with different rainfall rate thresholds (01/Jul/2016 - 31/May/2020).

was 0.02 for the default rainfall rate threshold value. A 40% increase in the $\bar{R}_{sat}$ from the default value resulted in an 18% decrease in $\bar{E}_c/\bar{R}$. Similarly, a 40% decrease from the default threshold resulted in a 19% increase in $\bar{E}_c/\bar{R}$. According to the results in Section 3.2 (Fig. 7c), a change of 20% in $\bar{E}_c/\bar{R}$ has negligible effect in interception losses (~1%). We used the 0.5 mm h^{-1} $\bar{R}_{sat}$ for the computation of $\bar{E}_c$ and $\bar{R}$ for the automatic model parameterization in Section 3.3.3.

3.3.2. Regression method

The best fit between the rainfall and throughfall data, as indicated by the highest average r^2 of the two regression lines, was achieved for a P_s value of 4 mm for all event-based intervals and daily data of the 01/Jul/2016 and 31/Dec/2018 period. The derived $\bar{E}_c/\bar{R}$ was negative for all event separation intervals (−0.05 - −0.15), as well as for the daily data (−0.14). This was caused by events or days where *TF* was greater than *P*, resulting in a slope of the R2 regression line above the 1:1 line. The observed daily *TF* was greater than *P* for 10 rain days (Fig. 11), with the maximum difference between *TF* and *P* observed on 09/Sep/2018 (4.7 mm). Scatter plots showed no relations between the *TF*/*P* fractions of the 28 manual *TF* gauges and the event rainfall, the number of gauges with *TF*>*P*, the wind speed, and the canopy fraction of the individual gauges (Supplementary material, Figs. S6 and S7). Thus, we considered the data to be representative. However, both *P* and *TF* observations could be affected by wind.

Using only rain days with previous dry days, the regression resulted even in an $\bar{E}_c/\bar{R}$ of −0.3. Excluding the events or days where *TF* is greater

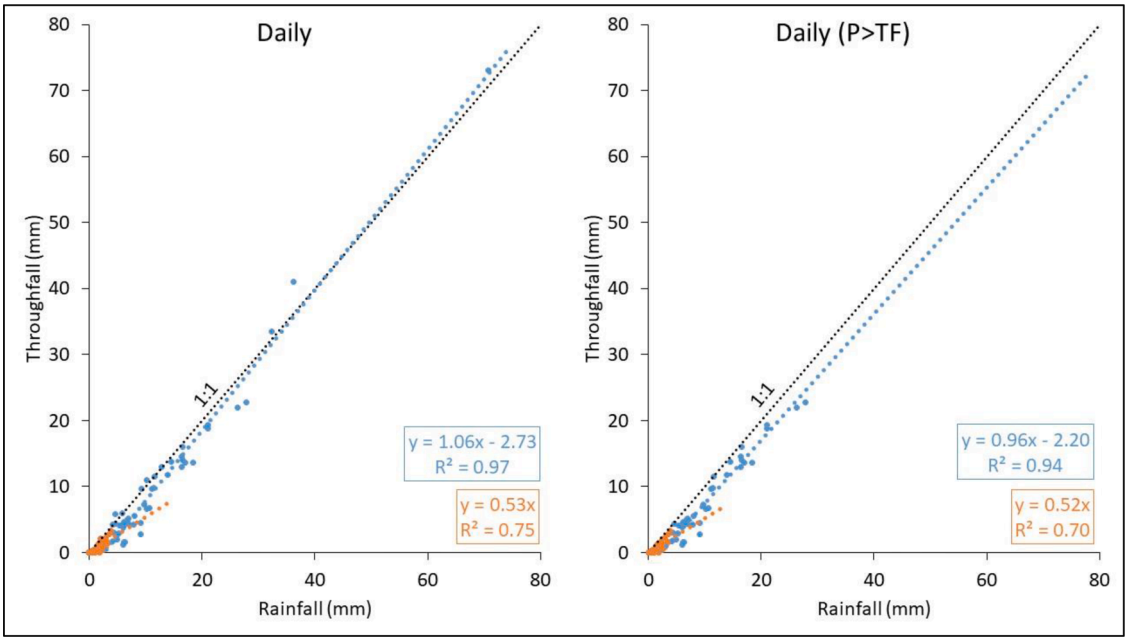

Fig. 11. The regression lines for rainfall events (01/Jul/2016 - 31/Dec/2018) that do not fill (orange) and fill (blue) the canopy storage (S), for the daily events with (left) and without (right) TF > P events.

than P resulted in a shift of the R2 line below the 1:1 line, which allowed the derivation of the $\bar{E}_c/\bar{R}$ (Table 4). The regression-derived $\bar{E}_c/\bar{R}$ (0.09) for daily events was higher than the computed $\bar{E}_c/\bar{R}$ (0.03) in Section 3.3.3.

The selection of different event separation intervals clearly affected all parameter values, illustrating again the equifinality of the models. For the 2-hour event separation interval, the higher $\bar{E}_c/\bar{R}$ value, which would increase interception, compared to the daily events, was counterbalanced with lower value of S, which would indeed reduce interception, whereas the value of c was the same. However, for the 6-hour and 12-hour event separation intervals, the higher $\bar{E}_c/\bar{R}$ values, compared to the daily events, were counterbalanced with lower values of both S and c, resulting in small differences in the computed I.

3.3.3. *Automatic model parameterization*

The observed interception losses were 18% of the rainfall for both the calibration and validation periods. The Rutter, Gash and Liu models showed high performance *(KGE* > 0.95*)* both for the calibration and validation period and both for *optimization-S,c* and *optimization-S* (Table 5). The regression method resulted in lower *KGE*s but still above 0.90. However, the 840 days without rain (see Section 3.1) contributed to the high values of the *KGE*s. The selection of a parameter set from different event separation interval (Table 4) resulted in different *KGE*'s and *P.BIAS* in Gash and Liu models. For example, the parameter set from the 6 hour event separation interval leads to lower model performance (0.84 *KGE* for Gash model and 0.88 *KGE* for Liu model) and to higher *P. BIAS* (−8.3% for Gash model and −3.7% for Liu model) than the parameter set derived from daily data.

The *P.BIAS* was slightly higher for the validation than for the calibration runs, but remained below 5% for all models and parameter derivation procedures. The sum of the absolute errors (*SAE*) showed also little difference between the models and parameterization procedures. The higher errors for the validation period, compared to the calibration period, can be related to the higher throughfall (26%). It could have been expected that fitting both S and c (*optimization-S,c*) would result in better calibration results and worse validation results, compared to the results obtained with only S fitted and c observed (*optimization-S*). However, the performance of the two automatic calibration procedures remained remarkably similar.

The canopy cover fraction (c) derived from the *optimization-S,c* (0.79 – 1.0) was higher than the observed c (0.69) for all models. The S ranged from 1.31 to 1.75 mm for the *optimization-S,c* method and from 1.38 to 2.13 mm for the *optimization-S* method. The regression method resulted in a lower c than the optimization methods, which was balanced by a higher S and $\bar{E}_c/\bar{R}$.

The increase in S with the decrease in c is due to equifinality, as is also illustrated by the *KGE* values from 400 test runs with the same S and c combinations as used in Section 3.2 (Supplementary material, Fig. S8). The number of S-c combinations for which the model performance exceeded a *KGE* of 0.95 was 129 for hourly Rutter, 124 for daily Rutter, 69 for Gash and 64 for Liu. The range of S values for which *KGE* was over 0.95 was highest for the hourly Rutter model (1.0 - 4.0 mm) and smallest for the Gash model (1.0 - 2.6 mm). The c values for these runs ranged between 0.3 and 1 for the hourly Rutter and Gash models and between 0.4 and 1 for the daily Rutter and Liu models.

The models showed similar daily errors (modelled minus observed throughfall) (Fig. 12). The highest positive error with the *optimization-S, c* method during the calibration period occurred during 9.2 mm daily rain with 2.8 mm observed throughfall; the error ranged between 4.8 mm (Liu) and 5.8 mm (daily Rutter). The highest negative error occurred during a 36.3 mm daily rain with 41.0 mm observed throughfall and ranged between –6.4 mm (daily Rutter) to −7.0 mm

Table 4
The number of rainfall events (N) after the exclusion of $TF > P$ events, canopy storage capacity (S), canopy cover fraction (c), ratio of wet canopy evaporation rate to rainfall rate ($\bar{E}_c/\bar{R}$) for three event-based rainfall separation intervals and for the daily data (Daily), derived using two regression lines (R1,R2) for the period between 01/Jul/2016 and 31/Dec/2018 (throughfall 545 mm) and the computed throughfall with the Gash model (TF_{Gash}).

Parameter	2 h	6 h	12 h	Daily
N	153	100	83	101
S (mm)	1.61	1.23	1.50	1.95
c	0.48	0.44	0.42	0.48
$\bar{E}_c/\bar{R}$	0.15	0.32	0.12	0.09
r^2 of R1	0.75	0.85	0.84	0.70
r^2 of R2	0.94	0.94	0.96	0.94
TF_{Gash} (mm)	518	497	540	520

Table 5
Measured rainfall (*P*) and throughfall (*TF*), model parameter values for the three models, the two optimization methods (*optimization-S, optimization-S,c*) and the regression method and the Kling-Gupta Efficiency (*KGE*), percent bias (*P.BIAS*) and sum of absolute error (*SAE*) for the calibration and validation periods (S = canopy storage capacity, c = canopy cover fraction, $\bar{E}_c/\bar{R}$ = mean evaporation to mean rainfall ratio).

	Optimization-S				*Optimization-S,c*				*Regression*	
	Rutter H	Rutter D	Gash	Liu	Rutter H	Rutter D	Gash	Liu	Gash	Liu
Calibration 01/07/2016 - 31/12/2018, P = 667.8 mm, TF = 544.9 mm										
S (mm)	1.85	2.13	1.38	1.58	1.49	1.75	1.31	1.38	1.95	1.95
c	0.69	0.69	0.69	0.69	0.88	1.00	0.79	0.93	0.48	0.48
$\bar{E}_c/\bar{R}$			0.03	0.03			0.03	0.03	0.09	0.09
TF (mm)	552	553	554	556	551	551	553	555	520	545
P.BIAS	1.4	1.6	1.6	2.1	1.2	1.0	1.5	1.8	−4.6	−0.1
KGE	0.960	0.962	0.955	0.949	0.961	0.970	0.956	0.950	0.901	0.923
SAE (mm)	99	102	98	97	99	100	98	97	102	102
Validation 01/01/2019 - 31/05/2020, P = 837.6 mm, TF = 686.5 mm										
TF (mm)	710	706	702	706	709	698	702	704	662	691
P.BIAS	3.5	2.8	2.2	2.9	3.2	1.7	2.2	2.5	−3.5	0.7
KGE	0.957	0.963	0.969	0.962	0.959	0.972	0.969	0.964	0.932	0.950
SAE (mm)	135	134	120	121	127	125	118	118	125	122

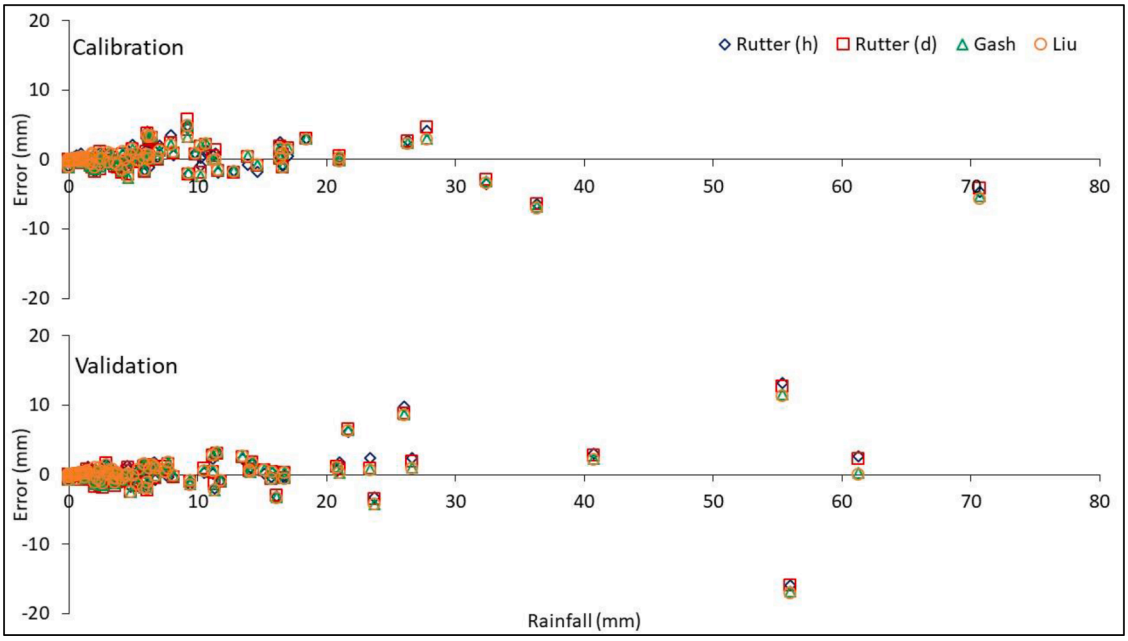

Fig. 12. Error (modelled minus observed throughfall) versus rainfall for the Rutter (hourly and daily), Gash and Liu models, for the calibration (01/Jul/2016 - 31/Dec/2018) and validation period (01/Jan/2019 - 31/May/2020), with the *optimization-S,c* parameter set.

(Liu). During validation the highest positive error ranged between 11.3 (Liu) and 13.1 mm (Rutter hourly during 55.4 mm rain with 41.3 mm observed throughfall. The highest negative error ranged between −17.2 mm (Liu) to −15.9 mm (Rutter hourly and daily) during 56 mm rain with 70.2 mm observed throughfall. Rainfall of these two validation events was similar but throughfall differed highly. Due to the relative small S (1.3 - 2.1 mm) and $\bar{E}_c/\bar{R}$ (0.03) or E_o (2.3 mm on average) the modelled daily interception values were less than 4 mm, while the observed interception ($I = P - TF$) ranged from −14.2 mm ($TF > P$) to 14.1 mm. The possible reasons for these large differences between the observed P and TF are discussed in Section 4.

The highest difference in the errors between the hourly and daily Rutter were observed during rainfall events that occur on consecutive days. For example, on 27/Feb/2019 we had 2.4 mm error for the hourly Rutter model with the *optimization-S,c* but only 0.9, 0.8 and 0.7 mm errors for the daily Rutter, Gash and Liu models, respectively,. Rainfall began on 26/Feb/2019 at 20:00 and ended on 27/Feb/2019 at 07:00. The water storage on the canopy (C_c) was zero at the end of day (26/Feb/2019) for the daily Rutter but reached 1.69 mm for the hourly Rutter. This amount of water was added on the next day's (27/Feb/2019) water balance, thus the difference between the hourly and the daily Rutter models.

3.4. Long-term model application (2008 – 2019)

The average number of rain days per year for the period 2008 – 2019 was 76 and the average annual P and E_o were 429 mm and 1457 mm, respectively (Supplementary material, Table S3). The observed I was, on average, 26% of P (Table 6) which is likely overestimated due to missing throughfall data (see Section 2.2.1). The computed interception losses were similar for all three models, both for *optimization-S* (18 – 19% of P) and for *optimization-S,c* (19 – 20% of P). The results are similar for the calibration and validation (Table 5), where we saw a slightly higher positive bias for throughfall, meaning lower interception, with *optimization-S* than with *optimization-S,c*. The pattern is consistent between years, with interception losses either the same or 1 to 3% higher for *optimization-S,c* than for *optimization-S*, for the individual models. The highest differences in the interception losses between the Gash and Liu models were in 2008 and 2009 (2 – 3% difference in I). The results indicate that the difference in I is due to the different behaviour of the

Table 6
Annual rainfall (P), annual average wet-day rain (Pn), annual rainfall for rain days less than 2 mm ($P_{<2}$) and interception (I) from the weekly observations and modelled with the Rutter (I_{Rutter}), Gash (I_{Gash}) and Liu (I_{Liu}) models, for the different parameter derivation methods. $P_{<2}$ and I are expressed as a fraction of P.

	Observed				*Optimization-S*			*Optimization-S,c*			*Regression*	
Year	P	Pn	$P_{<2}$	I	I_{Rutter}	I_{Gash}	I_{Liu}	I_{Rutter}	I_{Gash}	I_{Liu}	I_{Gash}	I_{Liu}
	mm	*mm/d*										
2008	186	4.2	0.10	0.55	0.24	0.23	0.21	0.27	0.24	0.22	0.25	0.21
2009	325	3.7	0.10	0.39	0.28	0.28	0.25	0.31	0.28	0.26	0.31	0.25
2010	475	8.5	0.03	0.13	0.12	0.13	0.13	0.13	0.14	0.13	0.17	0.15
2011	495	5.5	0.06	0.32	0.18	0.20	0.18	0.20	0.20	0.19	0.24	0.19
2012	560	5.8	0.06	0.19	0.19	0.20	0.19	0.21	0.21	0.20	0.25	0.20
2013	385	5.8	0.05	0.28	0.19	0.18	0.18	0.19	0.19	0.18	0.23	0.20
2014	381	5.8	0.05	0.24	0.21	0.19	0.18	0.22	0.19	0.18	0.23	0.19
2015	507	5.0	0.08	0.40	0.19	0.21	0.19	0.22	0.21	0.20	0.24	0.20
2016	359	4.3	0.06	0.25	0.22	0.23	0.22	0.24	0.23	0.22	0.29	0.23
2017	220	4.8	0.06	0.29	0.24	0.22	0.21	0.24	0.22	0.21	0.27	0.22
2018	575	7.2	0.04	0.17	0.15	0.16	0.16	0.16	0.16	0.16	0.21	0.17
2019	679	7.6	0.03	0.18	0.14	0.16	0.15	0.16	0.16	0.16	0.21	0.17
Av.	429	5.7	0.06	0.26	0.18	0.19	0.18	0.20	0.19	0.19	0.24	0.19

two models for the small rainfall events (before reaching saturation), as in the years 2008 and 2009 we had the highest percent contribution (10%) of rain days less than 2 mm. On the contrary, the difference in I between the two models was 0–1% in the years with lowest percent contribution (3 - 4%) of rain days less than 2 mm.

Higher interception losses (24% of P) were found for the Gash model with the use of the regression method derived parameters. On the contrary, interception losses with the Liu model were the same (19% of P) for *optimization-S, optimization-S,c* and the regression method. Large deviations between modelled and observed throughfall were found for the years 2008 and 2015, most likely due to missing throughfall data (see Section 2.2.1). For example, weekly throughfall was reported as 0 mm for a week with 37 mm rain on 22/May/2008 and for a week with 45 mm rain on 08/Oct/2015.

Relations between the observed P and the modelled I, showed a week correlation between the observed annual P and the modelled annual I for all three models (r^2: 0.35 – 0.49). We found, however, a strong negative relation between the average wet-day rain (Pn) and the Rutter (r^2 = 0.91), Gash (r^2 = 0.87) and Liu (r^2 = 0.90) modelled I. The Pn was computed as the total annual rainfall divided by the number of rain days ($P > 0$ mm). In 2010 we had the highest recorded daily rainfall (111.4 mm), the highest Pn (8.5 mm/d) and the lowest modelled$I$ (13 - 17%). In 2009 we had the lowest Pn (3.7 mm/d) and the lowest modelled I (25 - 31%).

4. Discussion

The values of the derived S, c, $\bar{E}$ and $\bar{R}$ parameters that have been reported in other studies on pine trees are presented in Table 7. Computed $\bar{E}/\bar{R}$ from meteorological data and from regression based derived $\bar{E}/\bar{R}$ and were found in an equal number of studies. The computed $\bar{E}_c/\bar{R}$ values for the different rainfall rate thresholds in our study were very small (0.01 to 0.04) and this fourfold increase has a small effect on the interception losses (~1% increase in I (% of P)). Gash

Table 7
Rainfall interception modelling studies on pine trees, the species studied and their location, the average annual rainfall (P) and Interception (I), the models applied (Mod: Ru=Rutter, Ga = Gash, Li = Liu), the parameter derivation procedure (superscript: R = regression-based, L = literature, M = measured, O = optimized) and the parameter values used for the canopy storage capacity (S), canopy cover fraction (c), computed wet evaporation ($\bar{E}$) and rainfall ($\bar{R}$) rates and the ratio $\bar{E}/\bar{R}$.

Study	Species	Location	P (mm)	I (% P)	Mod	S (mm)	c	$\bar{E}$ (mm h^{-1})	$\bar{R}$ (mm h^{-1})	$\bar{E}/\bar{R}$*
Rutter et al. (1971)	*P. nigra*	Southeast England		34 - 35	Ru	0.9 - 1.0^{R}	0.75^{R}			
Gash (1979)	*P. sylvestris*	East England		27	Ga	0.8^{L}	0.68 - 0.74^{L}	0.19	1.38	
Bringfelt and Lindroth (1987)	*P. sylvestris*	Sweden			Ru	0.48^{L}	0.41^{L}			
Loustau et al. (1992)	*P. pinaster*	France	920	14 - 22	Ga	0.50 - 0.55^{R}	0.40 - 0.45^{R}			0.06 - 0.11
Lankreijer et al. (1993)	*P. pinaster*	France		13	Ga	0.26^{R}	0.43^{R}	0.19	1.26	0.09
Gash et al. (1995)	*P. pinaster*	France		13	Ga	0.25^{R}	0.45^{R}	0.08	1.65	
Llorens (1997)	*P. sylvestris*	Spain		18	Ga	1.34$^{L, R}$	0.78$^{L, R}$	0.36	3.83	0.12
Valente et al. (1997)	*P. pinaster*	Portugal	600	16	Ru, Ga	0.41^{R}	0.64^{M}	0.32	1.74	
Bryant et al. (2005)	*P. palustris, P. taeda*	USA (Georgia)	830	18 - 22	Ga	0.98^{R}	0.88^{M}	0.1	2.03	
Carlyle-Moses and Price (2007)	*P. pseudostrobus* (Mixed forest)	Northeast Mexico	635	16	Ga, Li	2.4^{R}	0.5^{M}			0.19
Zhongjie et al. (2010)	*P. armandii*	China	592	14	Ga	2.86^{R}	0.64^{R}	0.17	1.99	
Licata et al. (2011)	*P. ponderosa*	Patagonia, Argentina	800	34 - 39	Ga	0.71–2.70$^{M, R}$	0.54 - 0.85^{R}			0.01 - 0.25
Buttle and Farnsworth (2012)	*P. resinosa*	Ontario, Canada	950	12 - 30	Li	0.85 - 1.03$^{\circ, R}$	0.52 - 0.80^{M}			0.05 - 0.14
Ghimire et al. (2012)	*P. roxburghii*	Central Nepal	1487	17	Ga	0.67^{R}	0.73^{R}	0.34	2.46	0.14
Návar (2013)	*P. pseudostrobus*	Mexico	640	18	Ga	1.03 ^{R}	0.74 ^{M}	0.76	11.87	0.09
Sadeghi et al. (2015)	*P. eldarica*	Northern Iran	272	27	Ga	1.24^{R}	0.62^{R}			0.07
Ma et al. (2019)	*P. tabuliformis*	China	580	24	Ga	1.38 −1.43^{R}	0.61 −0.63$^{M, R}$	0.03–0.06	0.82 - 1.83	0.11 - 0.13

*The ratio $\bar{E}/\bar{R}$ was derived with regression-based methods.

(1979) reported that an increase of 100% in the rainfall rate threshold resulted in a 15% decrease in $\bar{E}$ that led to 6% lower interception losses. However, the $\bar{E}/\bar{R}$ in their study was much higher (0.14). Similar low computed $\bar{E}$ values as in our study (0.01 – 0.05 mm h^{-1}) were found by Hörmann et al. (1996), for a beech forest in northern Germany. According to the authors, the low $\bar{E}$ values are due to the considerable rainfall events that took place during night hours. We also found that 43% of the total rainfall took place during the night hours.

The regression-derived $\bar{E}_c/\bar{R}$ value (0.09) is higher than the computed $\bar{E}_c/\bar{R}$ (see Section 3.3.2 – 3.3.3), but it is within the range of the values reported in the literature (Table 7). The higher regression-derived $\bar{E}/\bar{R}$ compared to the computed $\bar{E}/\bar{R}$ has been reported by other studies too (Ghimire et al., 2012; Hassan et al., 2017; Holwerda et al., 2012; Ghimire et al., 2017). According to Holwerda et al. (2012), possible reasons for the discrepancy between the computed and the regression-based $\bar{E}/\bar{R}$ are errors in *TF* measurements due to inadequate sampling design, the advection of sensible heat and the underestimation of the aerodynamic conductance. Previous studies have shown that the explicit use of fixed *TF* gauges, as done in our study, could result in an error of ~2% in throughfall measurements (Holwerda et al., 2006b; Lloyd and Marques, 1988). The computed $\bar{E}$ derived from the Penman-Monteith equation relies on the big leaf assumption, which abstracts the whole canopy into a one-layer source. This assumption is in conflict with the complex three dimensional structures of canopies (Luo et al., 2018). Also, the Penman-Monteith equation is valid for a large, uniform area, where evaporation can be considered a vertical process, thus advection is neglected (Valente et al., 1997).

Ringgaard et al. (2014) found that $\bar{E}$ estimates based on eddy covariance energy balance data (ECEB) are more robust than $\bar{E}$ estimates based on the Penman-Monteith equation. However. ECEB rates consist of evaporation from both canopy (E_c) and ground surface (E_s), meaning that the assumption of $E_c = E/c$ is only valid for zero E_s. Thus, the ECEB method is restricted to forest canopies with sufficient cover and zero evaporation from soil (or ground vegetation) during rain (Ringgaard et al., 2014). Comparing observed winter and summer interception and $\bar{E}$ estimates with the use of the revised Gash model, these authors found that advection may reach up to 50% of the available energy for evaporation during summer. Návar (2020) suggested that the correct physical interpretation of the role of the advected sensible heat flux in interception requires statistical equations that can be derived with data that include the measurement of *I* components across the full scope of common rainfall events in the forest of interest. The author found that in forests where advection of sensible heat flux is important, rainfall interception models in linear form redistribute $\bar{E}$ over the duration of the storm. On the contrary, models in power fashion forecast large $\bar{E}$ values early in the storm and decline rapidly as the storm progresses. The energy stored in the canopy and the early abatement appears to be more important in the latter process.

In the majority of the studies in Table 7, the parameters *S* and *c* are derived from regression based methods, while model optimization was applied only in one study (Buttle and Farnsworth, 2012). However, these authors optimized *S* only, while the current study optimizes *S* and *c* at the same time. A large range of values were found by the direct and indirect methods used to estimate *S* in different pine forests, because this parameter is controlled by many aspects of canopy structure, such as the basal area, the canopy height and the surface properties of foliage or wood area index (Carlyle-Moses and Gash, 2011; Llorens and Gallart, 2000). We found that an increase in the value of *S* with a parallel decrease in the value of *c* (or the opposite) results in the same model output, revealing equifinality between these parameters. Our results also confirm the findings of previous studies about equifinality between the parameters *S* and $\bar{E}/\bar{R}$ (Cisneros Vaca et al., 2018; van Dijk et al., 2015). The use of plant canopy observations for the estimation of *c* will eliminate the issues of equifinality in the optimization process. Our observed *LAI* value (2.38) is similar to the *LAI* value (2.57) reported by Fyllas et al. (2008) for *P. brutia* trees on the island of Lesvos (Greece).

The occurrence of events with more throughfall than rainfall constrains the use of the regression-based method for the derivation of model parameter values. The negative values for interception that we found amongst the rainfall and throughfall observations have been reported for a wide range of forest types and climates (Crockford and Richardson, 2000). High spatial and temporal variability in *TF*, including higher *TF* than *P*, can be linked with high wind speeds, variable rainfall droplet sizes, changes in the canopy cover due to damage by strong winds or pests, air moisture condensation or dripping points as a result of the canopy architecture (Calder, 1996; David et al., 2006; Grunicke et al., 2020; Holwerda et al., 2010; Klaassen et al., 1998; Van Dijk and Bruijnzeel, 2001a, 2001b; Xiao et al., 2000). These events can be linked also with hail storms (Supplementary material, Fig. S9). The selection of daily data for which *TF* is lower than *P* allowed the derivation of model parameter values with the regression-based method. The exclusion of $P\langle\ TF$ data implies that these data were not representative. However, we did not find relations between average and maximum wind speeds or canopy cover of individual throughfall gauges and *TF/P* fractions in our data set that would indicate this. One would expect that a throughfall record with a sufficiently long time series and a large number of gauges would be representative, while it would include throughfall observations that are either higher or lower than the actual throughfall. Thus, the selective removal of $TF \rangle\ P$ events for the model parameter derivation process could lead to an underestimation of throughfall and overestimation of interception.

The Gash model was chosen in the majority of rainfall interception modelling studies on pine trees, while the Rutter was applied only in three studies and all of them published before the year 2000 (Table 7). A key drawback of the Rutter model is the requirement of high temporal resolution of the input data (Muzylo et al., 2009). The daily application of the Rutter model tested in this study resulted in high model performance ($KGE > 0.95$) and small *P.BIAS* ($< 5\%$), similar to the Gash and Liu model. Thus, the daily Rutter model can be applied in areas where hourly data are not available. The main advantage of the daily Rutter model is that it relies on measured E_o values, while the Gash and Liu models use a single value of $\bar{E}/\bar{R}$ for the model application. Even though, the regression-method derived parameters are often used for the application of the Liu model, we should highlight that in the formulation of this model, the storage component behaves exponentially until reaching saturation and not linearly, as assumed with the regression method. If we would have used our observed c, $\bar{E}_c/\bar{R}$ and E_o and selected *S* values from studies conducted in similar climates and with trees with similar *c*, we could have picked either 0.41 (Valente et al., 1997) or 2.86 (Zhongjie et al., 2010) from Table 7. For *S* equal to 0.41 mm, interception losses were 5%, 8% and 7% of *P* for the daily Rutter, Gash and Liu model, respectively, whereas for *S* equal to 2.86 mm, interception losses were 20%, 29% and 24%. These results indicate the importance of throughfall measurements for interception model parameterization and seem to disagree with Limousin et al. (2008). These authors noted that *S* and $\bar{E}/\bar{R}$ values for a given tree species can be applied to other forests with the same species but different density, if measurements of *c* are made. On the contrary, Deguchi et al. (2006) reported that these parameters are very sensitive to changes in canopy structure and meteorological conditions.

A recently developed rainfall interception model named 'NvMx' (Návar, 2017) simplifies the estimation of forest interception by deriving separate parameters for throughfall and stemflow. The author showed that the mathematical functions of the rate of canopy storage and the rate of evaporation over time could take many forms depending on the forest, climate and rainfall conditions. Following up on these findings, Návar (2020, 2019) developed a method based on extended drip equations that provides independent and unbiased estimates of interception, canopy storage capacity and evaporation, as a function of precipitation or as a function of rainfall duration.

The interception losses observed in our study for the period 2016 – 2020 (18% of *P*) were within the range of the interception losses (17 –

29% of *P*) reported for *Pinus halepensis* trees in the Mediterranean (del Campo et al., 2018; Llorens and Domingo, 2007; Qubaja et al., 2020). The long-term application of the three daily interception models showed that the modelled interception was highly correlated to *Pn*. In their study on rainfall interception by an isolated evergreen *Quercus ilex* in Portugal, David et al. (2006) found that interception losses depend mostly on the distribution of rainfall in time, rather than the duration or the amount of rainfall. Thus, climates with frequent small storms and high evaporation rates will have the largest interception losses. In the context of climate change, the projected higher evapotranspiration rates will enhance interception loss. However, recent climate projections for the drier parts of the Mediterranean region show a 25% increase of extreme rainfall events (Zittis et al., 2021), which is expected to reduce the fraction of the intercepted rainfall.

5. Conclusion

This paper examines different parameter derivation approaches and model assumptions for the application of the hourly and daily Rutter interception model and the daily Gash and Liu models. The main conclusions drawn from this study are:

- The canopy related parameters (S and c) of the Rutter, Gash and Liu models show high relative sensitivity but also strong equifinality.
- Interception model parameters can be derived from throughfall data with the use of automatic optimization of S or both S and c, with evaporation derived from observations, as well as with the use of the regression method. We obtained low absolute P.BIAS (0.7%−3.5%) and high KGE (0.93–0.97) for the validation period (491 days) for all three parameter derivation methods and all four interception models.
- The derivation of model parameter values with the regression method is, however, not optimal, because it often involves a subjective selection of storm events and dry interval durations, which may result in different model parameter value sets. Selecting the parameter set from the 6 hour event separation interval leads to lower model performance (KGE $<$ 0.90) and to higher P.BIAS (−8.3% for Gash model and −3.7% for Liu model) than the parameter set derived from daily data.
- Model applications with c derived from plant canopy observations and S values from similar environments selected from the literature resulted in a large range of interception values (5% - 29%) around the observed 18% interception.
- A rainfall rate threshold of 0.5 mm $h-1$ has been commonly used to represent saturated canopy conditions for the computation of $\bar{E}c$ and $\bar{R}$. The use of different rainfall rate thresholds (0.1 – 1.4 mm $h-1$) had a minor effect on the interception losses of the Gash and Liu models. We found less than 1% change in interception losses for the period 01/Jul/2016 – 31/05/2020 (1505 mm rain).
- The application of the Rutter model with daily data, which we have not found in the literature, showed similar good performance as the hourly Rutter model and as the daily Gash and Liu models.
- High quality throughfall measurements are essential for the parameterization of rainfall interception models. Interception observed with 28 throughfall gauges during 2016–2020 was 18% of the rainfall. For the 2008–2019 period interception observed with 15 throughfall gauges was 26%. Incidentally missing throughfall data may have contributed to the high observed interception losses for the 2008 - 2019 period. The modelled interception for this twelve year period, obtained with the three daily models with the optimization-S, c parameter set, ranged between 19 and 20%. The modelled interception ranged between 12% and 31% for individual years and was related to the average wet day rainfall (Pn).
- Rainfall characteristics should be analysed to gain a better understanding of the interception process. We found that days with 2 mm rain and more amounted to 96.2% of the total rainfall for the period 2016 – 2020 and to 94.5% for the period 2008 – 2019, thus rainfall that saturate the canopy has a much higher effect on interception losses than small rainfall events that do not saturate the canopy.

Rainfall interception is a temporal and spatial variable process. Even though the assumptions of a dry canopy at the start of each day and a constant evaporation-rainfall ratio, as used by the daily application of the Gash and Liu model, do not confirm the reality, these models gave a good fit of the daily throughfall observations in an open Mediterranean pine forests. This was however associated with the strong parameter equifinality of these models. The Rutter model, which keeps a running water balance, gives a better description of the interception process, and the daily Rutter model obtained similar performance as the hourly model.

Declaration of Competing Interest

The authors declare that they have no known competing financial interests or personal relationships that could have appeared to influence the work reported in this paper.

Acknowledgments

We would like to express our sincere thanks to Corrado Camera, Elias Giannakis, Christos Zoumides, Ioannis Sofokleous, Melpomeni Siakou, Erkut Ulucam, Aitor Herrera and Kadidja Ahmed for their valuable help during field work. This research has received funding from the European Union's Horizon 2020 Research and Innovation programme, under Grant Agreement 641739 (BINGO Project) and from the Research and Innovation Foundation of Cyprus, through the Water Joint Programming Initiative, under Grant Agreement P2P/WATER/0218/0011 (FLUXMED project).

Supplementary materials

Supplementary material associated with this article can be found, in the online version, at doi:10.1016/j.agrformet.2021.108755.

References

Alavi, G., Jansson, P.E., Hällgren, J.E., Bergholm, J., 2001. Interception of a dense spruce forest, performance of a simplified canopy water balance model. Nord. Hydrol. 32, 265–284 https://doi.org/10.2166/nh.2001.0016.

Allen, R.G., Pereira, L.S., Raes, D., Smith, M., 1998. FAO Irrigation and Drainage Paper No.56 Crop Evapotranspiration, FAO. ISBN: 92-5-104219-5.

Beven, K.J., 2012. Rainfall-runoff modelling : the Primer. Wiley-Blackwell.

Bouten, W., Schaap, M.G., Aerts, J., Vermetten, A.W.M., 1996. Monitoring and modelling canopy water storage amounts in support of atmospheric deposition studies. J. Hydrol. 181, 305–321 https://doi.org/10.1016/0022-1694(95)02907-9.

Bringfelt, B., Lindroth, A., 1987. Synoptic evapotranspiration model applied to two northern forests of different density. J. Hydrol. 95, 185–201 https://doi.org/10.1016/0022-1694(87)90001-1.

Bryant, M.L., Bhat, S., Jacobs, J.M., 2005. Measurements and modeling of throughfall variability for five forest communities in the southeastern US. J. Hydrol. 312, 95–108 https://doi.org/10.1016/j.jhydrol.2005.02.012.

Buttle, J.M., Farnsworth, A.G., 2012. Measurement and modeling of canopy water partitioning in a reforested landscape: the Ganaraska Forest, southern Ontario. Canada. J. Hydrol. 103–114, 466–467https://doi.org/10.1016/j.jhydrol.2012.08.021.

Calder, I.R., 1996. 1 . Development of the two-layer stochastic model. J. Hydrol. 185, 363–378 https://doi.org/10.1016/0022-1694(86)90143-5.

Camera, C., Bruggeman, A., Hadjinicolaou, P., Pashiardis, S., Lange, M.A., 2014. Evaluation of interpolation techniques for the creation of gridded daily precipitation (1 × 1km 2); Cyprus, 1980-2010. J. Geophys. Res. Atmos. 119, 693–712 https://doi.org/10.1002/2013JD020611.

Carlyle-Moses, D.E., Gash, J.H.C., 2011. Rainfall Interception Loss By Forest Canopies. Springer, Dordrecht, pp. 407–423 https://doi.org/10.1007/978-94-007-1363-5_20.

Carlyle-Moses, D.E., Price, A.G., 2007. Modelling canopy interception loss from a Madrean pine-oak stand, northeastern Mexico. Hydrol. Process. 21, 2572–2580 https://doi.org/10.1002/hyp.6790.

Cisneros Vaca, C., van der Tol, C., Ghimire, C.P., 2018. The influence of long-term changes in canopy structure on rainfall interception loss: a case study in Speulderbos, the Netherlands. Hydrol. Earth Syst. Sci. 22, 3701–3719 https://doi.org/10.5194/hess-22-3701-2018.

Clarke, N., Zlindra, D., Ulrich, E., Mosello, R., Derome, J., Derome, K., König, N., Lövblad, G., Draaijers, G.P.J., Hansen, K., Thimonier, A., Waldner, P., 2016. Methods and criteria for harmonized sampling, assessment, monitoring and analysis of the effects of air pollution on forests. Part XIV: Sampling and Analysis of Deposition, ICP Forests.

Crockford, R.H., Richardson, D.P., 2000. Partitioning of rainfall into throughfall, stemslow and interception: effect of forest type, ground cover and climate. Hydrol. Process. 14, 2903–2920 https://doi.org/10.1002/1099-1085(200011/12)14:16/17<2903::AID-HYP126>3.0.CO;2-6.

David, T.S., Gash, J.H.C., Valente, F., Pereira, J.S., Ferreira, M.I., David, J.S., 2006. Rainfall interception by an isolated evergreen oak tree in a Mediterranean savannah. Hydrol. Process. 20, 2713–2726 https://doi.org/10.1002/hyp.6062.

Deguchi, A., Hattori, S., Park, H.T., 2006. The influence of seasonal changes in canopy structure on interception loss: application of the revised Gash model. J. Hydrol. 318, 80–102 https://doi.org/10.1016/j.jhydrol.2005.06.005.

del Campo, A.D., González-Sanchis, M., Lidón, A., Ceacero, C.J., García-Prats, A., 2018. Rainfall partitioning after thinning in two low-biomass semiarid forests: impact of meteorological variables and forest structure on the effectiveness of water-oriented treatments. J. Hydrol. 565, 74–86 https://doi.org/10.1016/j.jhydrol.2018.08.013.

Department of Forests of Cyprus, 2006. Criteria and Indicators for the Sustainable Forest Management in Cyprus [WWW Document] Dep. For. Minist. Agric. Nat. Resour. Environ. Nicosia,Cyprus. URL. http://www.moa.gov.cy/moa/fd/fd.nsf/C6778230A38A7472C2257E4D00325A62/$file/L079.pdf.

Eliades, M., Bruggeman, A., Lubczynski, M.W., Christou, A., Camera, C., Djuma, H., 2018a. The water balance components of Mediterranean pine trees on a steep mountain slope during two hydrologically contrasting years. J. Hydrol. 562, 712–724 https://doi.org/10.1016/j.jhydrol.2018.05.048.

Eliades, N.-.G., Aravanopoulos, F., Christou, A., Eliades, N.-G.H., Aravanopoulos Phil, F., Christou, A., A.K, 2018b. Mediterranean Islands Hosting Marginal and Peripheral Forest Tree Populations: the Case of Pinus brutia Ten. in Cyprus. Forests 9 514 https://doi.org/10.3390/f9090514.

Fernandes, R.P., Silva, R.W.da C., Salemi, L.F., Andrade, T.M.B.de, Moraes, J.M.de, Dijk, A.I.J.M.V., Martinelli, L.A., 2017. The influence of sugarcane crop development on rainfall interception losses. J. Hydrol. 551, 532–539 https://doi.org/10.1016/j.jhydrol.2017.06.027.

Ferretti, M., Fischer, R., Mues, V., Granke, O., Lorenz, M., 2010. Basic design principles for the ICP Forests Monitoring Networks.

Friesen, J., Lundquist, J., Van Stan, J.T., 2015. Evolution of forest precipitation water storage measurement methods. Hydrol. Process. 29, 2504–2520 https://doi.org/10.1002/hyp.10376.

Fyllas, N.M., Dimitrakopoulos, P.G., Troumbis, A.Y., 2008. Regeneration dynamics of a mixed Mediterranean pine forest in the absence of fire. For. Ecol. Manage. 256, 1552–1559 https://doi.org/10.1016/J.FORECO.2008.06.046.

Fylstra, D., Lasdon, L., Watson, J., Waren, A., 1998. Design and use of the Microsoft Excel Solver. Interfaces (Providence). https://doi.org/10.1287/inte.28.5.29.

Gash, J.H.C., 1979. An analytical model of rainfall interception by forests. Q. J. R. Meteorol. Soc. 105, 43–55 https://doi.org/10.1002/qj.49710544304.

Gash, J.H.C., Lloyd, C.R., Lachaud, G., 1995. Estimating sparse forest rainfall interception with an analytical model. J. Hydrol. 170, 79–86 https://doi.org/http://dx.doi.org/10.1016/0022-1694(95)02697-N.

Ghimire, C., Adrian Bruijnzeel, L., Lubczynski, M.W., Ravelona, M., Zwartendijk, B.W., van Meerveld, H.J.J.I., 2017. Measurement and modeling of rainfall interception by two differently aged secondary forests in upland eastern Madagascar. J. Hydrol. 545, 212–225 https://doi.org/10.1016/j.jhydrol.2016.10.032.

Ghimire, C.P., Bruijnzeel, L.A., Lubczynski, M.W., Bonell, M., 2012. Rainfall interception by natural and planted forests in the Middle Mountains of Central Nepal. J. Hydrol. 475, 270–280 https://doi.org/10.1016/j.jhydrol.2012.09.051.

Grunicke, S., Queck, R., Bernhofer, C., 2020. Long-term investigation of forest canopy rainfall interception for a spruce stand. Agric. For. Meteorol. 108125, 292–293 https://doi.org/10.1016/j.agrformet.2020.108125.

Hassan, S.M.T., Ghimire, C.P., Lubczynski, M.W., 2017. Remote sensing upscaling of interception loss from isolated oaks: sardon catchment case study. Spain. J. Hydrol. https://doi.org/10.1016/j.jhydrol.2017.08.016.

Holwerda, F., Bruijnzeel, L.A., Muñoz-Villers, L.E., Equihua, M., Asbjornsen, H., 2010. Rainfall and cloud water interception in mature and secondary lower montane cloud forests of central Veracruz. Mexico. J. Hydrol. 384, 84–96 https://doi.org/10.1016/j.jhydrol.2010.01.012.

Holwerda, F., Bruijnzeel, L.A., Scatena, F.N., Vugts, H.F., Meesters, A.G.C.A., 2012. Wet canopy evaporation from a Puerto Rican lower montane rain forest: the importance of realistically estimated aerodynamic conductance. J. Hydrol. 414, 1–15 https://doi.org/10.1016/j.jhydrol.2011.07.033.

Holwerda, F., Scatena, F.N., Bruijnzeel, L.A., 2006a. Throughfall in a Puerto Rican lower montane rain forest: a comparison of sampling strategies. J. Hydrol. 327, 592–602 https://doi.org/10.1016/J.JHYDROL.2005.12.014.

Holwerda, F., Scatena, F.N., Bruijnzeel, L.A., 2006b. Throughfall in a Puerto Rican lower montane rain forest: a comparison of sampling strategies. J. Hydrol. 327, 592–602 https://doi.org/10.1016/j.jhydrol.2005.12.014.

Hörmann, G., Branding, A., Clemen, T., Herbst, M., Hinrichs, A., Thamm, F., 1996. Calculation and simulation of wind controlled canopy interception of a beech forest in Northern Germany. Agric. For. Meteorol. 79, 131–148 https://doi.org/10.1016/0168-1923(95)02275-9.

Jackson, I.J., 1975. Relationships between rainfall parameters and interception by tropical forest. J. Hydrol. 24, 215–238 https://doi.org/10.1016/0022-1694(75)90082-7.

Kimmins, J.P., 1973. Some Statistical Aspects of Sampling Throughfall Precipitation in Nutrient Cycling Studies in British Columbian Coastal Forests. Ecology 54, 1008–1019 https://doi.org/10.2307/1935567.

Klaassen, W., Bosveld, F., de Water, E., 1998. Water storage and evaporation as constituents of rainfall interception. J. Hydrol. 36–50, 212–213https://doi.org/10.1016/S0022-1694(98)00200-5.

Kool, D., Agam, N., Lazarovitch, N., Heitman, J.L., Sauer, T.J., Ben-Gal, A., 2014. A review of approaches for evapotranspiration partitioning. Agric. For. Meteorol. 184, 56–70 https://doi.org/10.1016/j.agrformet.2013.09.003.

Lankreijer, H.J.M., Hendriks, M.J., Klaassen, W., 1993. A comparison of models simulating rainfall interception of forests. Agric. For. Meteorol. 64, 187–199 https://doi.org/10.1016/0168-1923(93)90028-G.

LI-COR Inc.,, 2017. LAI-2200C Plant Canopy Analyzer: Instruction manual, Instruction manual.

Licata, J.A., Pypker, T.G., Weigandt, M., Unsworth, M.H., Gyenge, J.E., Fernández, M.E., Schlichter, T.M., Bond, B.J., 2011. Decreased rainfall interception balances increased transpiration in exotic ponderosa pine plantations compared with native cypress stands in Patagonia. Argentina. Ecohydrology 4, 83–93 https://doi.org/10.1002/eco.125.

Limousin, J.M., Rambal, S., Ourcival, J.M., Joffre, R., 2008. Modelling rainfall interception in a mediterranean Quercus ilex ecosystem: lesson from a throughfall exclusion experiment. J. Hydrol. 357, 57–66 https://doi.org/10.1016/j.jhydrol.2008.05.001.

Linhoss, A.C., Siegert, C.M., 2020. Calibration reveals limitations in modeling rainfall interception at the storm scale. J. Hydrol. 124624 https://doi.org/10.1016/j.jhydrol.2020.124624.

Linhoss, A.C., Siegert, C.M., 2016. A comparison of five forest interception models using global sensitivity and uncertainty analysis. J. Hydrol. 538, 109–116 https://doi.org/10.1016/J.JHYDROL.2016.04.011.

Liu, S., 2001. Evaluation of the Liu model for predicting rainfall interception in forests world-wide. Hydrol. Process. 15, 2341–2360 https://doi.org/10.1002/hyp.264.

Liu, S., 1997. A new model for the prediction of rainfall interception in forest canopies. Ecol. Modell. 99, 151–159 https://doi.org/10.1016/S0304-3800(97)01948-0.

Llorens, P., 1997. Rainfall interception by a Pinus sylvestris forest patch overgrown in a Mediterranean mountainous abandoned area II. Assessment of the applicability of Gash's analytical model. J. Hydrol. 199, 346–359 https://doi.org/10.1016/S0022-1694(96)03335-5.

Llorens, P., Domingo, F., 2007. Rainfall partitioning by vegetation under Mediterranean conditions. A review of studies in Europe. J. Hydrol. 335, 37–54 https://doi.org/10.1016/j.jhydrol.2006.10.032.

Llorens, P., Gallart, F., 2000. A simplified method for forest water storage capacity measurement. J. Hydrol. 240, 131–144 https://doi.org/10.1016/S0022-1694(00)00339-5.

Lloyd, C.R., Marques, A.D.O., 1988. Spatial variability of throughfall and stemflow measurements in Amazonian rainforest. Agric. For. Meteorol. 42, 63–73 https://doi.org/10.1016/0168-1923(88)90067-6.

Loustau, D., Berbigier, P., Granier, A., 1992. Interception loss, throughfall and stemflow in a maritime pine stand. II. An application of Gash's analytical model of interception. J. Hydrol. 138, 469–485 https://doi.org/10.1016/0022-1694(92)90131-E.

Luo, X., Chen, J.M., Liu, J., Black, T.A., Croft, H., Staebler, R., He, L., Arain, M.A., Chen, B., Mo, G., Gonsamo, A., McCaughey, H., 2018. Comparison of Big-Leaf, Two-Big-Leaf, and Two-Leaf Upscaling Schemes for Evapotranspiration Estimation Using Coupled Carbon-Water Modeling. J. Geophys. Res. Biogeosci. 123, 207–225 https://doi.org/10.1002/2017JG003978.

Ma, C., Li, X., Luo, Y., Shao, M., Jia, X., 2019. The modelling of rainfall interception in growing and dormant seasons for a pine plantation and a black locust plantation in semi-arid Northwest China. J. Hydrol. 577 https://doi.org/10.1016/j.jhydrol.2019.06.021.

Ma, C., Luo, Y., Shao, M., 2020. Comparative modeling of the effect of thinning on canopy interception loss in a semiarid black locust (Robinia pseudoacacia) plantation in Northwest China. J. Hydrol. 590, 125234 https://doi.org/10.1016/j.jhydrol.2020.125234.

Monteith, J.L., 1965. Evaporation and environment. Symp. Soc. Exp. Biol. 19, 205–234.

Muzylo, A., Llorens, P., Valente, F., Keizer, J.J., Domingo, F., Gash, J.H.C., 2009. A review of rainfall interception modelling. J. Hydrol. 370, 191–206 https://doi.org/10.1016/j.jhydrol.2009.02.058.

Mużyło, A., Valente, F., Domingo, F., Llorens, P., 2012. Modelling rainfall partitioning with sparse Gash and Rutter models in a downy oak stand in leafed and leafless periods. Hydrol. Process. 26, 3161–3173 https://doi.org/10.1002/hyp.8401.

Návar, J., 2020. Modeling rainfall interception loss components of forests. J. Hydrol. 584, 124449 https://doi.org/10.1016/j.jhydrol.2019.124449.

Návar, J., 2019. Modeling rainfall interception components of forests: extending drip equations. Agric. For. Meteorol. 279, 107704 https://doi.org/10.1016/j.agrformet.2019.107704.

Návar, J., 2017. Fitting rainfall interception models to forest ecosystems of Mexico. J. Hydrol. 548, 458–470 https://doi.org/10.1016/j.jhydrol.2017.03.025.

Návar, J., 2013. The performance of the reformulated Gash's interception loss model in Mexico's northeastern temperate forests. Hydrol. Process. 27, 1626–1633 https://doi.org/10.1002/hyp.9309.

Pereira, F.L., Gash, J.H.C., David, J.S., David, T.S., Monteiro, P.R., Valente, F., 2009. Modelling interception loss from evergreen oak Mediterranean savannas: application of a tree-based modelling approach. Agric. For. Meteorol. 149, 680–688 https://doi.org/10.1016/j.agrformet.2008.10.014.

Qubaja, R., Amer, M., Tatarinov, F., Rotenberg, E., Preisler, Y., Sprintsin, M., Yakir, D., 2020. Partitioning evapotranspiration and its long-term evolution in a dry pine forest

using measurement-based estimates of soil evaporation. Agric. For. Meteorol. 281, 107831 https://doi.org/10.1016/j.agrformet.2019.107831.
Ringgaard, R., Herbst, M., Friborg, T., 2014. Partitioning forest evapotranspiration: interception evaporation and the impact of canopy structure, local and regional advection. J. Hydrol. 517, 677–690 https://doi.org/10.1016/J.JHYDROL.2014.06.007.
Rodrigo, A., Àvila, A., 2001. Influence of sampling size in the estimation of mean throughfall in two Mediterranean holm oak forests. J. Hydrol. 243, 216–227 https://doi.org/10.1016/S0022-1694(00)00412-1.
Rutter, A.J., Kershaw, K.A., Robins, P.C., Morton, A.J., 1971. A predictive model of rainfall interception in forests, 1. Derivation of the model from observations in a plantation of Corsican pine. Agric. Meteorol. 9, 367–384 https://doi.org/http://dx.doi.org/10.1016/0002-1571(71)90034-3.
Sadeghi, S.M.M., Attarod, P., Van Stan, J.T., Pypker, T.G., Dunkerley, D., 2015. Efficiency of the reformulated Gash's interception model in semiarid afforestations. Agric. For. Meteorol. https://doi.org/10.1016/j.agrformet.2014.10.006.
Schellekens, J., Scatena, F., Bruijnzeel, L., Wickel, A., 1999. Modelling rainfall interception by a lowland tropical rain forest in northeastern Puerto Rico. J. Hydrol. 225, 168–184 https://doi.org/10.1016/S0022-1694(99)00157-2.
Shachnovich, Y., Berliner, P.R., Bar, P., 2008. Rainfall interception and spatial distribution of throughfall in a pine forest planted in an arid zone. J. Hydrol. 349, 168–177 https://doi.org/10.1016/j.jhydrol.2007.10.051.
Shuttleworth, W.J., Gurney, R.J., 1990. The theoretical relationship between foliage temperature and canopy resistance in sparse crops. Q. J. R. Meteorol. Soc. 116, 497–519 https://doi.org/10.1002/qj.49711649213.
Stewart, J.B., 1977. Evaporation from the wet canopy of a pine forest. Water Resour. Res. 13, 915–921 https://doi.org/10.1029/WR013i006p00915.
Valente, F., David, J.S., Gash, J.H., 1997. Modelling interception loss for two spares eucalyopt and pine forests in central Portugal unssing reformulated Rutter and Gash analytical models. J. Hydrol. 190, 141–162 https://doi.org/10.1016/S0022-1694(96)03066-1.
Van Dijk, A.I.J.M., Bruijnzeel, L.A., 2001a. Modelling rainfall interception by vegetation of variable density using an adapted analytical model. Part 1. Model description. J. Hydrol. 247, 230–238 https://doi.org/10.1016/S0022-1694(01)00392-4.
Van Dijk, A.I.J.M., Bruijnzeel, L.A., 2001b. Modelling rainfall interception by vegetation of variable density using an adapted analytical model. Part 2. Model validation for a tropical upland mixed cropping system. J. Hydrol. 247, 239–262 https://doi.org/10.1016/S0022-1694(01)00393-6.
van Dijk, A.I.J.M., Gash, J.H., van Gorsel, E., Blanken, P.D., Cescatti, A., Emmel, C., Gielen, B., Harman, I.N., Kiely, G., Merbold, L., Montagnani, L., Moors, E., Sottocornola, M., Varlagin, A., Williams, C.A., Wohlfahrt, G., 2015. Rainfall interception and the coupled surface water and energy balance. Agric. For. Meteorol 214 (215), 402–415 https://doi.org/10.1016/j.agrformet.2015.09.006.
Wallace, J., McJannet, D., 2008. Modelling interception in coastal and montane rainforests in northern Queensland. Australia. J. Hydrol. 348, 480–495 https://doi.org/10.1016/J.JHYDROL.2007.10.019.
Wei, L., Qiu, Z., Zhou, G., Zuecco, G., Liu, Y., Wu, Z., 2020. Rainfall interception recovery in a subtropical forest damaged by the great 2008 ice and snow storm in southern. China. J. Hydrol. 590, 125232 https://doi.org/10.1016/j.jhydrol.2020.125232.
Xiao, Q., McPherson, E.G., Ustin, S.L., Grismer, M.E., 2000. A new approach to modeling tree rainfall interception. J. Geophys. Res. Atmos. 105, 29173–29188 https://doi.org/10.1029/2000JD900343.
Zhongjie, S., Yanhui, W., Lihong, X., Wei, X., Pengtao, Y., Jixi, G., Linbo, Z., 2010. Fraction of incident rainfall within the canopy of a pure stand of Pinus armandii with revised Gash model in the Liupan Mountains of China. J. Hydrol. 385, 44–50 https://doi.org/10.1016/j.jhydrol.2010.02.003.
Zittis, G., Bruggeman, A., Lelieveld, J., 2021. Revisiting future extreme precipitation trends in the Mediterranean. Weather Clim. Extrem. 34, 100380 https://doi.org/10.1016/J.WACE.2021.100380.